

Environment Canada

Water Science and Technology Directorate

Direction générale des sciences et de
la technologie, eau
**Environnement
Canada**

TD
226
N87
no.08-266

**A Wealth of Water; Wise
Management of Watersheds,
Lakes and River Systems**

**R. P. Bukata, C. E. Binding, J. H. Jerome,
W. G. Booty & J. Lawrence**

WSTD Contribution No. 08-266

A Wealth of Water; Wise Management of Watersheds, Lakes and River Systems

R. P. Bukata, C. E. Binding, J. H. Jerome,
W. G. Booty & J. Lawrence



An Environment Canada CSA-sponsored GRIP project

March 2008

*Aquatic Ecosystem Management Research Division
Water Science and Technology Directorate
Science and Technology Branch
Environment Canada
867 Lakeshore Rd.
Burlington, ON, L7R 4A6*



Environment
Canada

Environnement
Canada

A Wealth of Water; Wise Management of Watersheds, Lakes and River Systems

R.P. Bukata, C.E. Binding, J.H. Jerome, W.G. Booty and J. Lawrence

NWRI RESEARCH SUMMARY

Plain language title

A Wealth of Water; Wise Management of Watersheds, Lakes and River Systems –
FINAL REPORT

What is the problem and what do scientists already know about it?

Remote sensing of coastal and inland waters for the determination of water quality is a complex problem requiring a thorough understanding of the interaction between each of the main colour producing agents and visible light entering the water column. For several decades, scientists at NWRI have completed theoretical studies to determine the optical properties of the main colour producing agents in the Great Lakes and developed radiative transfer models appropriate to optically complex waters for the derivation of water quality parameters from aquatic colour.

Why did NWRI do this study?

The Canadian Space Agency funded GRIP program Wealth of Water (WOW), was initiated in order to further develop and validate methods for the extraction of water quality parameters from aquatic colour, and produce remotely sensed water quality products for the Great Lakes that may be of consequence to environmental stewards.

What were the results?

The WOW project made significant advancements in the application of remote sensing technologies to environmental monitoring of the Great Lakes, producing observations of water quality (including water clarity, suspended particulates and algal blooms) that directly contribute to Environment Canada's mandates to monitor and protect freshwater quality.

How will these results be used?

Having confirmed the ability to use remote sensing imagery for the purpose of monitoring changes in water quality in the Great Lakes, such remote sensing products may be more readily incorporated into water quality monitoring programs of Canadian inland waters.

Who were our main partners in the study?

Canadian Space Agency, Department of Fisheries and Oceans, Borstad Associates Ltd.

Abstract

The Canadian Space Agency funded GRIP project 'Wealth of Water' aimed to integrate remote sensing imagery of aquatic colour, ground-based water quality and optical surveys and data-sets of terrestrial land use, in order to assess water quality of the lower Great Lakes and the interaction between water quality and activities within the watershed. Remote sensing of water quality, achievable through the application of optical models and algorithms to remotely-sensed aquatic colour data, provides a means of examining water quality conditions on a near-continuous and lake-wide basis offering the potential for timely support in the monitoring and mitigation of adverse ecosystem impacts from, for example, local event-driven processes such as storm plumes, or recurring processes such as algal blooms. With the ongoing availability of SeaWiFS, MODIS and MERIS imagery (and proposed future sensors Sentinel-3 and VIIRS), aquatic colour data exists on the temporal and spatial scales required of such monitoring. The work carried out under the GRIP project 'Wealth of Water' (WOW) made significant advancements in the application of remote sensing technologies to routine environmental monitoring of the Great Lakes, producing observations of water quality that directly contribute to Environment Canada's mandates to monitor and protect freshwater quality. The water quality parameters produced and interpreted during WOW, and presented in this report are, water clarity, total suspended particulate matter, and algal blooms. These water quality parameters were derived through a combination of simple empirical approaches, inverse modelling and multivariate statistical methods. The development, modification, validation and application of bio-geo-optical models for the extraction of water quality parameters from satellite-measured aquatic colour was a major component of the project and required accurate determinations of the optical cross-section spectra of the main colour-producing agents found within the Great Lakes watershed. Results are presented that document the variability in these optical properties and the incorporation of these coefficients into specific modeling procedures for the retrieval of mineral sediments and algal blooms from aquatic colour. The GRIP WOW project has developed the capacity for image processing of moderate resolution satellite data from sensors such as MODIS and SeaWiFS, producing the daily, biweekly and monthly composite spectral water-leaving radiance data required as inputs into these models and algorithms. The research being carried out under this study is the first of its kind to combine the state-of-the-art scientific methods developed at NWRI for the determination of watercolour from satellite imagery with the study of the impacts of extreme events on stream chemistry using non-point source models. The research has indicated that extreme events can impact drinking water intake zones over large areas of Lake Ontario, including the development of algal blooms. Land-based activities and events can now be related to specific water quality issues that occur over large scales in lakes.

L'eau : une richesse – la sage gestion des bassins hydrographiques, des lacs et des rivières

R.P. Bukata, C.E. Binding, J.H. Jerome, W.G. Booty et J. Lawrence

Sommaire des recherches de l'INRE

Titre en langage clair

L'eau : une richesse – sage gestion des bassins hydrographiques, des lacs et des rivières – RAPPORT FINAL

Quel est le problème et que savent les chercheurs à ce sujet?

La télédétection des eaux côtières et intérieures pour déterminer la qualité de l'eau représente un problème complexe nécessitant une connaissance approfondie de l'interaction entre les principaux agents colorants et la lumière visible pénétrant dans la colonne d'eau. Depuis des dizaines d'années, les scientifiques de l'INRE effectuent des études théoriques pour déterminer les propriétés optiques des principaux agents colorants dans les Grands Lacs. Pour ce faire, ils ont élaboré des modèles du transfert radiatif convenant aux eaux ayant des propriétés optiques complexes afin d'établir des paramètres de la qualité de l'eau à partir du spectre des couleurs de l'eau.

Pourquoi l'INRE a-t-il effectué cette étude?

Le programme « L'eau : une richesse », financé par les Initiatives gouvernementales en observation de la Terre (IGOT) de l'Agence spatiale canadienne, a été mis en place pour affiner et valider les méthodes d'extraction des paramètres de la qualité de l'eau à partir des couleurs de l'eau et pour développer des produits de télédétection de la qualité de l'eau dans les Grands Lacs, ce qui peut présenter un intérêt pour les responsables en matière de gérance de l'environnement.

Quels sont les résultats?

Le projet « L'eau : une richesse » a permis de réaliser d'importants progrès dans l'application des technologies de télédétection à la surveillance environnementale dans les Grands Lacs, en produisant des observations sur la qualité de l'eau (incluant la clarté de l'eau, les particules en suspension et la prolifération des algues) qui contribuent directement au mandat d'Environnement Canada de surveiller et de protéger la qualité des eaux douces.

Comment ces résultats seront-ils utilisés?

La capacité d'utilisation de l'imagerie de télédétection pour surveiller les changements dans la qualité de l'eau des Grands Lacs étant maintenant indéniable, ces produits peuvent être intégrés plus facilement dans les programmes de surveillance de la qualité des eaux intérieures du Canada.

Quels étaient nos principaux partenaires dans cette étude?

Agence spatiale canadienne, Pêches et Océans Canada, Borstad Associates Ltd.

Résumé

L'Agence spatiale canadienne a financé le projet « L'eau : une richesse », qui relève des Initiatives gouvernementales en observation de la Terre (IGOT). Ce projet vise à combiner l'imagerie de télédétection du spectre des couleurs de l'eau, des relevés au sol de la qualité et des propriétés optiques de l'eau et des ensembles de données sur l'utilisation des terres, afin d'évaluer la qualité de l'eau dans le réseau des Grands Lacs inférieurs et l'interaction entre la qualité de l'eau et les activités dans le bassin hydrologique. La télédétection de la qualité de l'eau, effectuée grâce à l'application d'algorithmes et de modèles optiques aux données télédéteectées sur la couleur de l'eau, permet d'examiner les conditions de la qualité de l'eau sur une base presque continue et à l'échelle d'un lac. Cette méthode offre également la possibilité d'un appui ponctuel pour la surveillance et l'atténuation des impacts néfastes sur l'écosystème induits, par exemple, par des processus découlant d'événements locaux tels que les panaches de sédiments après le passage d'une tempête ou des processus récurrents, comme la prolifération des algues. Avec la disponibilité des technologies d'imagerie SeaWiFS, MODIS et MERIS (et les capteurs Sentinel-3 et VIIRS proposés), des données sur la couleur de l'eau sont disponibles à l'échelle temporelle et spatiale requise pour une telle surveillance. Les travaux menés dans le cadre du projet « L'eau : une richesse » des IGOT a permis de grandes avancées dans l'application des technologies de télédétection à la surveillance environnementale régulière des Grands Lacs, produisant des observations de la qualité de l'eau qui contribuent directement au mandat d'Environnement Canada de surveiller et de protéger la qualité des eaux douces. Les paramètres de la qualité de l'eau interprétés dans le cadre du projet « L'eau : une richesse », et présentés dans le présent rapport, sont la clarté de l'eau, les particules totales en suspension et la prolifération des algues. Ces paramètres résultent d'une combinaison de stratégies empiriques simples, de rétro-modélisation et de méthodes statistiques multidimensionnelles. L'élaboration, la modification, la validation et l'application des modèles bio-géo-optiques pour extraire des paramètres de la qualité de l'eau à partir des couleurs de l'eau mesurées par un satellite ont été les éléments majeurs du projet et ont exigé une détermination précise des spectres de la section efficace optique des agents colorants observés dans le bassin hydrologique des Grands Lacs. Les résultats présentés étayent la variabilité des propriétés optiques et l'incorporation de ces coefficients dans des procédures de modélisation spécifiques pour extraire les sédiments minéraux et la prolifération des algues à partir de la couleur de l'eau. Le projet « L'eau : une richesse » des IGOT a également permis d'améliorer le traitement des images satellitaires à résolution moyenne provenant de capteurs tels que MODIS et SeaWiFS, qui produisent de façon quotidienne, bimensuelle et mensuelle des données spectrales composites de la radiance de l'eau servant d'entrées dans les modèles et les algorithmes. Les recherches entreprises dans le cadre de cette étude sont les premières dans le domaine à combiner les méthodes scientifiques à la fine pointe de la technologie qui ont été élaborées à l'INRE pour expliquer les couleurs de l'eau à partir de l'imagerie satellitaire et étudier les impacts des phénomènes extrêmes sur la chimie des cours

d'eau à l'aide de modèles de sources diffuses. Les recherches ont permis d'établir que les phénomènes extrêmes, y compris la prolifération des algues, peuvent avoir une incidence sur les zones d'approvisionnement en eau potable dans de grands secteurs du lac Ontario. On peut maintenant associer des activités et des événements terrestres à des problèmes particuliers concernant la qualité de l'eau qui s'étendent à de grandes portions des lacs.

TABLE OF CONTENTS

TABLE OF CONTENTS.....	0
LIST OF TABLES.....	2
LIST OF FIGURES.....	2
EXECUTIVE SUMMARY.....	4
1 INTRODUCTION.....	5
1.1 Project Objectives.....	6
2 DATA ACQUISITION.....	8
2.1 APPARENT OPTICAL PROPERTIES.....	8
2.2 INHERENT OPTICAL PROPERTIES.....	9
2.2.1 ABSORPTION.....	9
2.2.2 PARTICULATE SCATTERING.....	14
3 SATELLIE IMAGE ACQUISITION & PROCESSING.....	16
3.1 IMAGE PROCESSING.....	16
3.2 IMAGE ARCHIVE.....	17
4 WATER QUALITY REMOTE SENSING; MODELLING, VALIDATION & APPLICATIONS.....	18
4.1 A SIMPLE ASSESSMENT OF WATER CLARITY CHANGE IN THE GREAT LAKES.....	18
4.2 INVERSE MODELLING OF MODIS RED/NIR WAVEBANDS FOR THE MONITORING OF SUSPENDED PARTICULATES.....	23
4.3 INVERSE MODELLING OF MODIS RED/NIR WAVEBANDS FOR THE MONITORING OF ALGAL BLOOMS.....	29
5 RELATING WATER QUALITY TO LAND USE IN THE GREAT LAKES WATERSHED - Lake Ontario Watershed Loadings.....	34
5.1 UNIT AREA LOADS METHOD.....	35
5.2 EVENT MEAN CONCENTRATIONS METHOD.....	36
5.3 MEASURED FLOWS AND CHEMISTRY METHODS.....	37
5.4 NON-POINT SOURCE LOAD MODELLING.....	38
6 COMMUNICATIONS.....	42
7 THE FUTURE.....	43
8 SUMMARY & CONCLUSIONS.....	44
REFERENCES.....	45
APPENDICES.....	48

LIST OF TABLES

Table 1: Key Project Activities and Expected Results.....	7
Table 2: Research Cruise Details.....	8
Table 3: Range and spectral variation of the ratio $a_{NAP}(\lambda):[SPM]$ ($m^2 g^{-1}$). Coefficient of variation (CoV) determined as the percentage standard deviation as a fraction of the mean.	11
Table 4: Range and spectral variation of a_{ph} ($m^2 mg^{-1}$). Coefficient of variation (CoV) determined as the percentage standard deviation as a fraction of the mean.	13
Table 5: Aquatic colour satellite image archive for the Great Lakes region.....	17
Table 6: Least square regression coefficients of the form $Zs=\alpha nLw^\beta$ for data sets of in situ Secchi disk depth (Zs) and coincident satellite nLw_{550}	20
Table 7: Correlation coefficients between MODIS red and NIR water-leaving reflectance ratios (R_1/R_2) and SPM concentrations. Shaded regions indicate correlations with reflectance at a single wavelength.....	23
Table 8: Model parameters.....	25
Table 9: Unit Area load coefficients for various land uses.....	35
Table 10: Winter et al. 2002 unit area load coefficients.....	35
Table 11: PLUARG 1975-77 average unit area loads.....	35

LIST OF FIGURES

Figure 1: Schematic describing the process of deriving water quality products from remotely sensed aquatic colour.	6
Figure 2: Examples of particulate absorption spectra for various stations in Lake Erie. Spectra show total particulate absorption, a_p , non-algal particles, a_{NAP} , as measured after bleaching with sodium hypochlorite, and phytoplankton absorption, a_{ph} , as determined by subtracting a_{NAP} from a_p . All spectra are corrected under the assumption of zero absorption at 740:750 nm.....	10
Figure 3: (a) Absorption spectra of non-algal particulates (a_{NAP}) normalized to a_{NAP} at 440 nm for all stations sampled, (b) ratio of a_{NAP} at 350 to 440 nm versus percentage matter lost on ignition confirming steeper slopes of a_{NAP} are associated with more inorganic suspended matter.....	12
Figure 4: Phytoplankton specific absorption coefficients with spectra normalized to the absorption coefficient at 440 nm. Data is taken over a range of $a_{CDOM}(440)$ illustrating the apparent increase in phytoplankton absorption over blue wavelengths with increasing a_{CDOM}	13
Figure 5: Relationship between $a_{CDOM}(440)$ and the spectral slope of its absorption (S_{CDOM}).	14
Figure 6: Variation of b_{MSS} and b_{SPM} (estimated from $b_{T(660)}/[MSS]$ and $b_{T(660)}/[SPM]$ respectively) with organic fraction of suspended particulate matter determined through Loss On Ignition.	15
Figure 7: Spectral scattering measured in Lake Ontario using the AC9. Spectra normalized to scattering at 555 nm.....	15
Figure 8: (a) Average CZCS nLw_{550} for the period 1979-1985, (b) average SeaWiFS nLw_{555} for the period 1998-2005 and (c) difference between the two images.....	19
Figure 9: Secchi disk depth (Zs) against coincident SeaWiFS nLw_{555} and CZCS nLw_{550} during surveys on (a) Lake Erie and (b) Lake Ontario. Least square regression equations of the form $Zs=\alpha nLw^\beta$ are presented in table 1.	20

Figure 10: Average Lake Erie Secchi disk depth (meters) for the periods (a) 1979-1985 and (b) 1998-2005 and (c) change in Secchi depth between the two periods.	21
Figure 11: Average Lake Ontario Secchi disk depth (meters) for the periods (a) 1979-1985 and (b) 1998-2005 and (c) change in Secchi depth between the two periods.	22
Figure 12: Measured TSM concentrations versus those modelled from MODIS nLw748.....	25
Figure 13: MODIS-estimated biweekly lake-wide mean Water Column (WC) SPM concentrations, and W^3 (wind speed cubed) obtained from Lake Erie buoyed weather stations.	27
Figure 14: Monthly mean distribution of total water column SPM ($g\ m^{-2}$) derived from inverse modelling of MODIS nLw748.	28
Figure 15: Agreement between in situ [chl _a] and that predicted from MODIS through inverse modeling assuming a C_{667} of 0.025.	30
Figure 16: Algal bloom flag before correction for erroneous cloud/ice edge pixels. Red pixels indicating inferred chlorophyll concentrations greater than $15\ mg\ m^{-3}$	31
Figure 17: Normalised spectral water-leaving radiance for typical algal dominated waters flagged as chlorophyll > $15\ mg\ m^{-3}$ (pink) and those erroneous pixels flagged in winter (blue).32	
Figure 18: Percentage reduction in pixels flagged as having chlorophyll concentration greater than $15\ mg\ m^{-3}$ following nLw531<nLw551 condition.	32
Figure 19: Algal bloom flag after correction for erroneous cloud/ice edge pixels. Red pixels indicating inferred chlorophyll concentrations greater than $15\ mg\ m^{-3}$	33
Figure 20: Lake Ontario Quaternary watersheds.....	34
Figure 21: Example unit area load calculations for Bronte Creek.....	36
Figure 22: Event mean concentration annual total phosphorus loads for the period 1980-2005..	37
Figure 23: Duffins Creek Total Phosphorus Monthly EMC Loadings	37
Figure 24: Niagara River TP loadings using the Beale and NWRI load estimate methods.	38
Figure 25: Comparison of various storm event scenarios for phosphorus loadings.....	39
Figure 26: Comparison of baseline and Aug. 19 2005 storm phosphorus loads predicted using ROS/AGNPS model.	39
Figure 27: Comparison of baseline and Aug. 19 2005 storm nitrogen loads predicted using ROS/AGNPS model.	40
Figure 28: Comparison of baseline and Aug. 19 2005 storm total suspended solids loads predicted using ROS/AGNPS model.	40
Figure 29: MODIS nLw555 imagery indicating general turbidity in Lake Ontario before and after the August 19 th storm event.	41

EXECUTIVE SUMMARY

The Canadian Space Agency funded GRIP project 'Wealth of Water' aimed to integrate remote sensing imagery of aquatic colour, ground-based water quality and optical surveys and data-sets of terrestrial land use, in order to assess water quality of the lower Great Lakes and the interaction between water quality and activities within the watershed. Remote sensing of water quality, achievable through the application of optical models and algorithms to remotely-sensed aquatic colour data, provides a means of examining water quality conditions on a near-continuous and lake-wide basis offering the potential for timely support in the monitoring and mitigation of adverse ecosystem impacts from, for example, local event-driven processes such as storm plumes, or recurring processes such as algal blooms. With the ongoing availability of SeaWiFS, MODIS and MERIS imagery (and proposed future sensors Sentinel-3 and VIIRS), aquatic colour data exists on the temporal and spatial scales required of such monitoring.

The work carried out under the GRIP project 'Wealth of Water' (WOW) made significant advancements in the application of remote sensing technologies to routine environmental monitoring of the Great Lakes, producing observations of water quality that directly contribute to Environment Canada's mandates to monitor and protect freshwater quality. The water quality parameters produced and interpreted during WOW, and presented in this report are:

- **Water Clarity (Secchi Depth)** – relevant to water quality perception, algal bloom dynamics (including benthic algal mats), monitoring effects of invasive species
- **Total Suspended Particulate Matter (SPM)** – important for monitoring shoreline erosion/accretion, lake dynamics, contaminant transport
- **An Algal Bloom flag**, based on estimated chlorophyll concentrations – of use in detecting the onset, and monitoring the progress, of algal blooms and relevant to studies of related toxins, taste and odour events, beach closures and water treatment plant operations

These water quality parameters were derived through a combination of simple empirical approaches, inverse modelling and multivariate statistical methods. The development, modification, validation and application of bio-geo-optical models for the extraction of water quality parameters from satellite-measured aquatic colour was a major component of the project and required accurate determinations of the optical cross-section spectra of the main colour-producing agents found within the Great Lakes watershed. Results are presented that document the variability in these optical properties and the incorporation of these coefficients into specific modeling procedures for the retrieval of mineral sediments and algal blooms from aquatic colour. The GRIP WOW project has developed the capacity for image processing of moderate resolution satellite data from sensors such as MODIS and SeaWiFS, producing the daily, biweekly and monthly composite spectral water-leaving radiance data required as inputs into these models and algorithms.

The research being carried out under this study is the first of its kind to combine the state-of-the-art scientific methods developed at NWRI for the determination of water colour from satellite imagery with the study of the impacts of extreme events on stream chemistry using non-point source models. The research has indicated that extreme events can impact drinking water intake zones over large areas of Lake Ontario, including the development of algal blooms. Land-based activities and events can now be related to specific water quality issues that occur over large scales in lakes.

1 INTRODUCTION

Aquatic resources within the Great Lakes watershed have been impacted over the years by numerous environmental stressors as a consequence of, for example, farming practices, shipping, urbanization and industrialization. The introduction of non-native invasive species, point-source discharges, nutrient loading and resulting eutrophication and nuisance algal blooms have all led to notable fluctuations in water quality and clarity (Environment Canada, 2001). Earth observation satellites have a logical place in the monitoring of water quality within the Great Lakes watershed, providing regular, high resolution coverage of the region that may present more robust evidence of spatial and temporal trends in water quality than intermittent point-sampling alone. As such, the project 'Wealth of Water' aims to produce remotely sensed water quality products of consequence to Environmental stewardship that enable both the assessment of water quality in the Great Lakes and give insight to the interactions between water quality and land use activities within the watershed.

The spectral variation of visible radiation leaving a water body, as seen from a remote platform such as an aircraft or satellite sensor, provides information suitable for the detection of colour-producing water quality parameters such as phytoplankton pigments, mineral suspended particulates, and dissolved organic matter. It has long been understood that the visible radiation upwelling from a natural water body is dictated by the inherent optical properties (IOPs) of the main colour producing agents (CPAs) residing within that water body. Thus, reliable interpretation of satellite measurements of water colour in terms of water quality is also dependent upon a thorough understanding of the spectral absorption and scattering properties pertinent to the water body under consideration. Due to the comparatively simple optical configuration of Case-1 waters, single-CPA models and algorithms based upon determinations of phytoplankton IOPs (e.g., Morel and Prieur, 1977; Morel and Loisel, 1998) have performed satisfactorily in oceanic waters. In contrast, Case-2 water optical properties are very often dominated by the effects of land-derived suspended inorganic particulates and dissolved organic matter that often neither co-vary with phytoplankton nor each other. Due to the additional number of organic and inorganic CPAs present in Case-2 waters and the potentially large variability in the inherent optical properties of each of these CPAs, models and algorithms based solely upon chlorophyll-bearing biota are invalid when applied to inland and coastal waters (Bukata et al., 1981; 1995; Bowers et al., 1996; Babin et al., 2003).

Figure 1 shows a simplified schematic depicting the process of deriving water quality products from remotely sensed aquatic colour imagery. The process first requires the accurate removal of atmospheric effects, correction for interactions at the air-water interface and removal of suspect data through stringent data quality controls and flagging. Scientists at NWRI have over several decades used bio-geo-optical modeling procedures coupled with in situ optical monitoring to develop novel approaches for extracting water quality information from water colour observations in optically complex waters (Bukata et al., 2005, Bukata et al., 1995). It is these previously developed methodologies, along with some modified and new methodologies, that are applied to remotely-sensed aquatic colour data to extract the water colouring parameters and produce maps of water quality over Canadian inland waters.

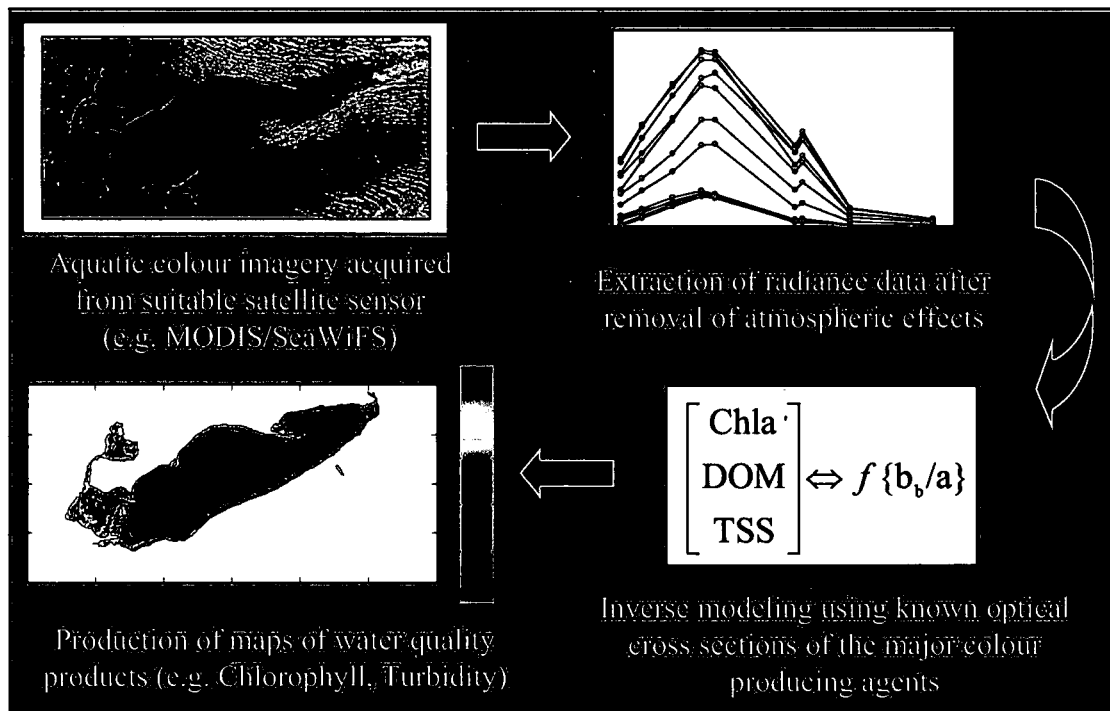


Figure 1: Schematic describing the process of deriving water quality products from remotely sensed aquatic colour.

1.1 Project Objectives

The main objectives of the project are:

- Through field-work obtain the inherent optical properties (IOPs) of the chlorophyll, suspended particulates, and dissolved organic carbon indigenous to Lakes Ontario and Erie.
- Develop new, and modify existing models and methodologies to enable the extraction of water quality from aquatic colour.
- Generate maps of water quality over the Great Lakes from remotely sensed aquatic colour.
- Where and when possible, from satellite data, observe algal blooms within the Great Lakes.
- Through data analyses and model integration via RAISON develop GIS outputs of land-use/water quality interactions for input into policies of environmental stewardship.

Key activities as outlined in the project work plan are shown in Table 1 including the expected results within each activity. This report is subsequently broken down into those key activities in order to deal specifically with the project goals and associated outcomes.

Table 1: Key Project Activities and Expected Results

Key Activity	Expected Results
Project management	Successful execution of the project to meet the goals set out in the agreement between EC and CSA.
Data acquisition	To compile comprehensive data sets of optical properties and WQ parameters for the lower great lakes
Satellite image acquisition & processing	Produce a dataset of suitable processed aquatic colour imagery including where possible processing to produce water quality products for the lower Great Lakes.
Data Analysis, modelling & assessment of WQ products	Optical properties of colour-producing agents on the lower Great Lakes. Derive water quality products from aquatic colour
Relating water quality to land use change	Report on land-use activities in the Lake Ontario watershed and their impacts on lake Ontario water quality with emphasis on large storm events.
Communications & Awareness	Generate interest in satellite monitoring of inland water quality at national and international levels of academe.

2 DATA ACQUISITION

A total of nine research cruises on board the *CCGS Limnos* were carried out between September 2004 and September 2007, visiting a total of 189 stations in Lakes Erie, Ontario and Winnipeg (Table 2). Stations provided a wide range of concentrations of the main colour producing agents and their associated inherent optical properties. Optical measurements carried out at each station included above- and in-water apparent optical properties, in-water inherent optical properties (using the WetLabs AC-9), fluorescence and attenuation properties.

Table 2: Research Cruise Details

Date	Lake	Stations
Sept 2004	Erie	25
May 2005	Erie	24
July 2005	Erie	27
Sept 2005	Erie	17
Apr 2006	Ontario	26
July 2006	Ontario	31
Oct 2006	Ontario	21
Jul 2007	Winnipeg	4
Sep 2007	Winnipeg	14
TOTAL:		189

At each station, water samples were obtained from the surface mixed layer and filtered for the determination of phytoplankton pigments (Chlorophyll *a* + phaeopigments, referred to as CHL from this point on), suspended particulates (total, inorganic, and organic fractions) and dissolved organic carbon (DOC) as well as laboratory determinations of selected inherent optical properties (CDOM & particulate spectral absorption). Concentrations of CHL were determined spectrophotometrically after extraction in acetone according to the methods of the National Laboratory for Environmental Testing, NLET (Environment Canada, 1997). Total concentrations of suspended particulate matter (SPM) were measured gravimetrically on pre-weighed Whatman GF/F filters after rinsing with distilled water. Organic matter lost on ignition (LOI) was determined after baking the filters for 3 hours at 500°C, giving the concentration of mineral suspended sediments (MSS) and, by subtraction, organic suspended sediments (OSS). DOC was determined by wet chemical oxidation according to the methods of NLET. CDOM absorption was measured spectrophotometrically after filtration through 0.2 µm membrane filters. Particulate absorption was measured using the quantitative filter technique after the concentration of particles on to Whatman GF/F filters (see Binding et al. 2008 for complete methodology for CDOM and particulate absorption analyses).

2.1 APPARENT OPTICAL PROPERTIES

The WATERS buoy, developed at NWRI to measure components of the incident and in-water light fields, was deployed to determine apparent optical properties at each station. The remote sensing reflectance was measured just beneath the surface by WATERS. Water colour imagers aboard various satellites attempt to estimate the remote sensing reflectance from their measurements of the upwelling light at satellite altitudes by correcting for impacts of the atmosphere. The rate of loss of downwelling light through the upper 4 m of the surface mixed

layer was also measured to obtain the irradiance attenuation coefficient. Combining these two apparent optical properties with the inherent optical property of total attenuation enables the calculation of the bulk absorption and scattering coefficients for the water mass and its constituents.

2.2 INHERENT OPTICAL PROPERTIES

Prior to this study only a limited catalogue of spectral IOPs from Canadian inland waters existed and further observations were needed in order to facilitate improvements in the accuracy of inverse modelling techniques for the retrieval of water quality products from aquatic colour. Inherent optical properties of aquatic CPAs can be effectively extracted from *in situ* observations of apparent optical properties (AOPs) using optical modelling procedures, can be measured in controlled laboratory experiments (e.g. the quantitative filter technique for absorption), or measured directly *in situ* using instruments such as the Wetlabs AC-9. Considering the optically complex nature of the Great Lakes waters, it would be reasonable to expect large variability in the IOPs of the main constituents. The aim of the work undertaken here was, therefore, to produce a data set of IOPs for the main CPAs present in the Great Lakes and obtain information regarding the natural variability of those coefficients which may subsequently be useful for improving the parameterization of optical models and remote sensing algorithms for the determination of water quality parameters over inland and coastal waters.

2.2.1 ABSORPTION

The absorption coefficients presented here were obtained through laboratory analyses of the quantitative filter technique (see Binding et al., 2008, for methods and complete analysis). One advantage of laboratory determinations of absorption coefficients is the ability to separate the main CPAs and study the natural variability of their absorption properties as a consequence of factors such as biogeochemical composition and concentration effects. At some stations, independent *in situ* absorption measurements were available from the Wetlabs AC-9 instrument and confirmed the accuracy of the filter-pad technique in measuring total absorption in these waters.

Total particulate absorption ($a_p(\lambda)$) was dominated by strong absorption in the blue portion of the visible spectrum, typical of mineral and/or detrital particles, with a clear chlorophyll *a* absorption peak at ~670 nm. The full range of a_p at 440 nm spanned 0.039 to 2.199 m^{-1} . Bleached particles produced absorption spectra that increased exponentially with decreasing wavelength. The resulting phytoplankton absorption spectra were highly variable, ranging from typical chlorophyll *a* spectra to exponentially increasing absorption at wavelengths shorter than 500 nm. Such atypical chlorophyll absorption spectra were most evident at stations with elevated CDOM absorption. Evidence was presented that suggests there was a fraction of particulate absorption which cannot be attributed to phytoplankton pigments, living heterotrophs, mineral sediments, or organic detritus but instead was indicative of a significant contribution from colloidal and/or particle-bound DOM.

Figure 2 presents example absorption spectra for total particulates, phytoplankton, and non-algal particles, measured at four stations within Lake Erie which exhibited a range of CDOM absorption, increasing from 0.1 m^{-1} in Fig. 2a to 0.4 m^{-1} in Fig. 2d. In Fig. 2a the phytoplankton absorption spectra is in agreement with the traditional spectral shape of absorption by chlorophyll-bearing phytoplankton. From Fig. 2b through to Fig. 2d, spectra show an increase in particulate absorption at short wavelengths, resulting in an apparent increase in phytoplankton absorption to

the degree that the known absorption peak at 440 nm is obscured. These observations of a consistent increase in measured particulate absorption with increasing CDOM may be supportive of a number of processes involving DOM such as its sorption onto particles or the presence of large colloidal DOM, both of which could be retained on filters and bleached during the quantitative filter technique resulting in erroneous elevations in the derived phytoplankton absorption.

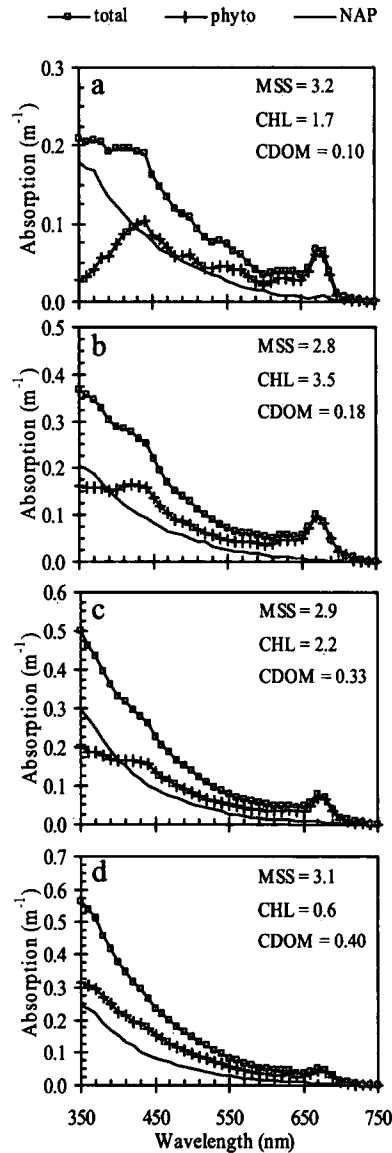


Figure 2: Examples of particulate absorption spectra for various stations in Lake Erie. Spectra show total particulate absorption, a_p , non-algal particles, a_{NAP} , as measured after bleaching with sodium hypochlorite, and phytoplankton absorption, a_{ph} , as determined by subtracting a_{NAP} from a_p . All spectra are corrected under the assumption of zero absorption at 740:750 nm.

Non-algal particulates

Non-algal particulates suspended in the water column may consist of mineral sediments, non-living organic detritus such as fecal matter and degrading phytoplankton cells, in addition to living non-algal organisms. In this study, absorption by the bleached particles (a_{NAP}) at 440 nm showed a strong linear relationship with the total concentration of suspended particulate matter (SPM), with a slope similar to those obtained by Bowers et al. (1996) and Babin et al. (2003) ($a_{\text{NAP}}(440) = 0.0214[\text{SPM}]$, $R^2 = 0.82$). The mean ratio $a_{\text{NAP}}(\lambda):[\text{SPM}]$, is presented in Table 3 for a selection of wavelengths. At 440 nm, the mean $a_{\text{NAP}}:[\text{SPM}]$ was $0.0403 \text{ m}^2 \text{ g}^{-1}$, with a variation about the mean of 76%. Babin et al. (2003) reported an average $a_{\text{NAP}}(443):[\text{SPM}]$ of $0.041 \text{ m}^2 \text{ g}^{-1}$ with a coefficient of variation of 56%.

The spectral absorption coefficients for non-algal particles in this study were described well by an exponential function according to Eq. 1.

$$a_{\text{NAP}}(\lambda) = a_{\text{NAP}}(440)e^{(-S_{\text{NAP}}(\lambda-440))} \quad (1)$$

The exponential slope (S_{NAP}) of the spectral absorption was determined for each station and resulted in a mean value of 0.011 nm^{-1} , with a range of 0.0077 to 0.017 nm^{-1} , which is in good agreement with those in the literature. In a wide range of European coastal waters Babin et al. (2003) reported NAP absorption coefficients with an average exponential slope of 0.0123 nm^{-1} , and a range of 0.0089 - 0.0178 nm^{-1} . Bowers et al. (1996) observed an exponential slope of 0.011 nm^{-1} for mineral dominated waters of the Irish Sea. The variability in the slope of NAP absorption can be seen clearly in Fig. 3a, where absorption spectra have been normalized to $a_{\text{NAP}}(440)$. This variability in the slope may be due to the wide range of particle types and relative proportions of mineral and organic matter found in the Lake Erie samples. Figure 3b shows the ratio of a_{NAP} at 350 to 440 nm, and despite significant scatter in the data, a clear decrease in the ratio can be seen with increasing organic content of the suspended matter.

Table 3: Range and spectral variation of the ratio $a_{\text{NAP}}(\lambda):[\text{SPM}]$ ($\text{m}^2 \text{ g}^{-1}$). Coefficient of variation (CoV) determined as the percentage standard deviation as a fraction of the mean.

Wavelength (nm)	400	440	490	510	550	670
Mean	0.057	0.040	0.025	0.019	0.012	0.003
Max	0.270	0.200	0.114	0.091	0.063	0.023
Min	0.021	0.013	0.007	0.006	0.004	0.000
CoV (%)	69.4	76.1	79.2	79.7	82.9	87.6

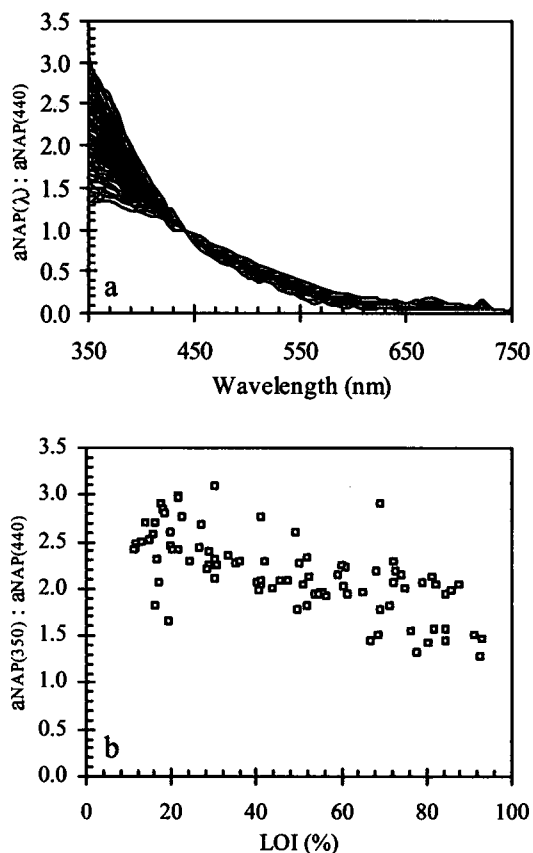


Figure 3: (a) Absorption spectra of non-algal particulates (a_{NAP}) normalized to a_{NAP} at 440 nm for all stations sampled, (b) ratio of a_{NAP} at 350 to 440 nm versus percentage matter lost on ignition confirming steeper slopes of a_{NAP} are associated with more inorganic suspended matter.

Phytoplankton

Phytoplankton absorption cross-sections, or chlorophyll-specific absorption coefficients, were taken simply as $\dot{a}_{ph}(\lambda) = a_{ph}(\lambda)/[CHL]$ for each filtered water sample and are presented in Table 4 for selected wavelengths. At 440 nm, \dot{a}_{ph} in this study reached a maximum of $0.505 \text{ m}^2 \text{ mg}^{-1}$, increasing to $0.617 \text{ m}^2 \text{ mg}^{-1}$ at 400 nm. These values are considerably higher than those previously published for marine and fresh-water phytoplankton (Bukata et al., 1991; Bricaud et al., 1995; Babin et al., 2003). Figure 4 shows spectral \dot{a}_{ph} normalized to \dot{a}_{ph} at 440 nm. The curves are average spectra taken over different ranges of measured CDOM absorption at 440 nm ($a_{CDOM}(440)$). The exponentially increasing absorption at short wavelengths usually associated with dissolved organic matter is clearly visible, particularly for $a_{CDOM}(440)$ greater than 0.2 m^{-1} .

Further work may be warranted to develop additional extraction techniques to remove DOM from the algal absorption signature before an accurate determination of algal spectral absorption can be made.

Table 4: Range and spectral variation of a_{ph}^* ($m^2 mg^{-1}$). Coefficient of variation (CoV) determined as the percentage standard deviation as a fraction of the mean.

Wavelength (nm)	400	440	490	510	550	670
Mean	0.087	0.086	0.050	0.040	0.029	0.040
Max	0.617	0.505	0.301	0.244	0.158	0.157
Min	0.009	0.013	0.005	0.007	0.004	0.007
CoV (%)	112.5	87.7	93.6	95.1	86.4	59.6

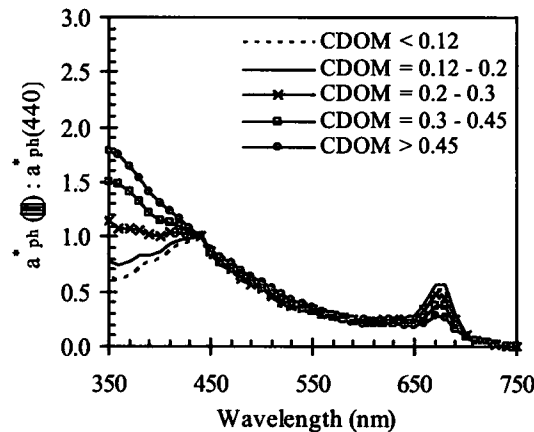


Figure 4: Phytoplankton specific absorption coefficients with spectra normalized to the absorption coefficient at 440 nm. Data is taken over a range of $a_{CDOM}(440)$ illustrating the apparent increase in phytoplankton absorption over blue wavelengths with increasing a_{CDOM} .

Dissolved Organic Matter

CDOM absorption at 440 nm ranged from 0.08 to 0.75 m^{-1} over the course of the study. The average specific absorption coefficient for dissolved organic carbon (DOC) at 440 nm ($a_{DOC}(440)$, calculated as $a_{CDOM}(440)/[DOC]$) in this study was 0.102 $m^2 g^{-1}$ and was in good agreement with the 0.115 $m^2 g^{-1}$ obtained by Bukata et al. (1983) for Lake Ontario. The slope of the spectral absorption of CDOM (S_{CDOM}) was in good agreement with those previously measured in coastal and inland waters, ranging from 0.0128 to 0.0197 nm^{-1} with a mean of 0.0161 nm^{-1} . Figure 9 presents the relationship between $a_{CDOM}(440)$ and S_{CDOM} . An inverse relationship can be seen for $a_{CDOM} < 0.2 m^{-1}$ ($R = -0.75$), in agreement with work of Carder et al. (1989), whereas for $a_{CDOM} > 0.2 m^{-1}$, there is a substantially more variable although significantly positive correlation ($R = 0.43$). The ranges of S_{CDOM} and a_{DOC} observed suggests that there may be large variations in the composition of the CDOM present in Lake Erie. The spectral slope of CDOM absorption has been shown to vary inversely with molecular weight, with high molecular weight humic acids exhibiting slopes less than 50% of the lower molecular weight fulvic acids (Zepp and Schlotzhauer, 1981; Carder et al., 1989). In addition, absorption by DOC increases with average molecular weight, with specific absorption of humic acid reported to be up to 24 times as large as that of fulvic acid (Carder et al., 1989; Kirk, 1994). High molecular weight DOM has been found to

preferentially adsorb onto mineral surfaces, leaving lower molecular weight components behind in solution, a process known as sorptive fractionation (Aufdenkampe et al., 2001; Shank et al., 2005). Given such selective removal of CDOM fractions, it is reasonable to expect that the bulk absorption properties of CDOM remaining in solution may be altered when significant adsorption onto particles occurs. The greater affinity of the higher molecular weight organic compounds to sediment surfaces suggests that relatively higher concentrations of the lower molecular weight compounds (exhibiting lower specific absorption and higher S_{CDOM}) may be evident in the residual CDOM during conditions leading to strong adsorption. The data distribution seen in Fig. 5 is in support of such a process occurring here.

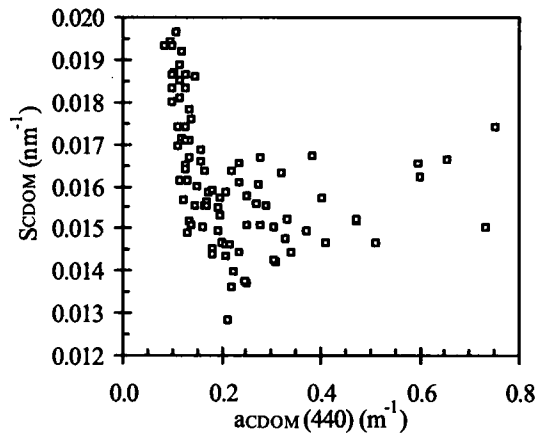


Figure 5: Relationship between $a_{CDOM}(440)$ and the spectral slope of its absorption (S_{CDOM}).

2.2.2 PARTICULATE SCATTERING

During Lake Erie surveys, neither AC9 measurements nor accurate in situ AOPs were available for determining scattering coefficients, therefore a single-wavelength (at 660 nm) total scattering coefficient (b_T) was estimated from the beam attenuation and filter absorption measurements at the same wavelength (by simple subtraction, $b = c - a_T$). At all stations, in situ measurements of transmittance were measured at 660 nm using a Wetlabs C-Star transmissometer. The beam attenuation coefficient, c , was derived from transmittance according to the relationship $T = e^{-cz}$ where z is the instrument pathlength (0.25m).

There was a strong correlation between the concentration of mineral sediments ([MSS]) and total particulate scattering at 660 nm ($b - b_w$) resulting in an average mineral-specific scattering coefficient of $0.751 \text{ m}^2 \text{ g}^{-1}$ (determined as the gradient of a regression of $b - b_w$ on [MSS]; $b - b_w = 0.741[\text{MSS}]$, $R^2 = 0.907$). This coefficient is high compared with documented coefficients for a range of coastal and inland waters. On closer inspection it was clear that the coefficient was elevated by the contribution to scattering from organic particles (phytoplankton cells, organic detrital matter, living heterotrophs etc). Figure 6 shows that b_{MSS}^* calculated as $(b - b_w)/[\text{MSS}]$ varies over an order of magnitude with increasing organic content of suspended particles (as represented by the % matter lost-on-ignition, LOI). Accounting for scattering by all particulate material by using [SPM] results in a lower b_{SPM}^* of $0.55 \text{ m}^2 \text{ g}^{-1}$ ($b - b_w = 0.554[\text{SPM}]$, $R^2 = 0.943$) with greatly reduced variability and no correlation with LOI. These scattering coefficients were

used in inverse modelling techniques to derive suspended particulate concentrations from MODIS in Lake Erie (section 4.2).

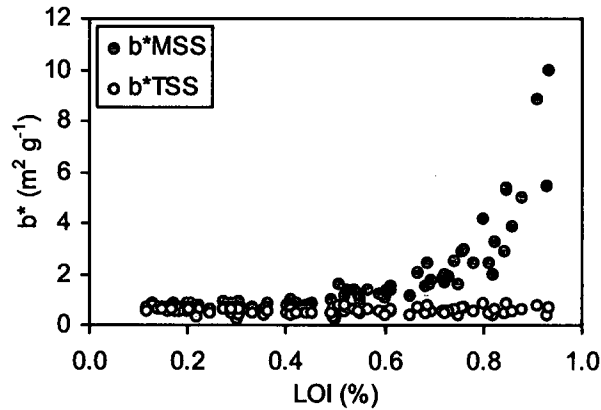


Figure 6: Variation of b^*_{MSS} and b^*_{SPM} (estimated from $b_T(660)/[MSS]$ and $b_T(660)/[SPM]$ respectively) with organic fraction of suspended particulate matter determined through Loss On Ignition.

In the Lake Ontario surveys the AC9 provided spectral scattering data that showed significant spectral variations in scattering (Figure 7) which may be attributed to variability in the size and composition of the suspended particles. Further analysis of AC9 and modelled scattering coefficients from AOP data is required for a more thorough understanding of full spectrum particulate scattering and determination of spectral scattering cross-section spectra for algal and mineral particulates in the Great Lakes.

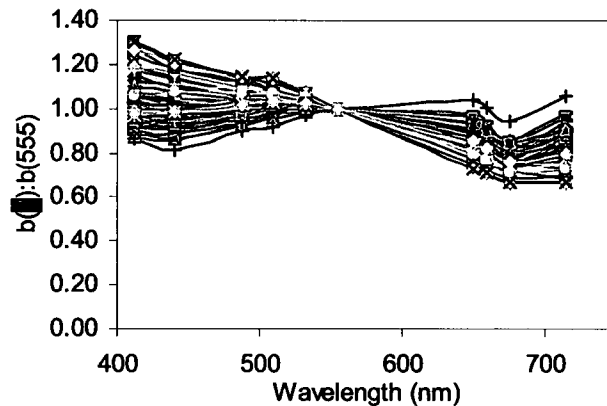


Figure 7: Spectral scattering measured in Lake Ontario using the AC9. Spectra normalized to scattering at 555 nm.

3 SATELLIE IMAGE ACQUISITION & PROCESSING

3.1 IMAGE PROCESSING

Imagery acquired and analyzed in this study were from the satellite sensors SeaWiFS, MODIS, CZCS, MERIS and Landsat. A dedicated image processing workstation was installed and successfully operated for the duration of the project for the acquisition, processing and interpretation of imagery. Details of image formats and processing are described below for each data source.

MODIS

A subscription was set up with the NASA Ocean Color Web Facility (<http://oceancolor.gsfc.nasa.gov/>) whereby daily L1A MODIS data granules for the Great Lakes region were made available via FTP. Imagery was processed using the dedicated ocean colour processing software SeaDAS v5.0 (Baith *et al.*, 2001). Code was written (combining SeaDAS, IDL and UNIX) in order to automatically download these files on a daily basis and process the L1A files through the stages of geolocation, subsetting and atmospheric correction to level-2 data generation. Normalized water-leaving radiance at the wavelengths 412, 443, 490, 512, 551, 665, 681, 705, 748 and 869 nm were produced for the region encompassed by 40-50°N, 74-94°W. Further processing including spatial and temporal binning produced L3 daily, biweekly, monthly, and annual composite images at 2km spatial resolution. Potentially erroneous pixels corresponding to conditions including land, cloud or ice, sun glint, saturated signals, and atmospheric correction failure were flagged and subsequently removed from further data analysis. Daily, biweekly and Monthly composites at 551 nm were mapped using an equal-area conic albers projection and exported in portable network graphic (.png) image format. Daily L1A and L2 data files and daily, biweekly and monthly L3 composite data files and images are archived for the period 2003 to present and image acquisition and processing is ongoing.

SeaWiFS

Monthly and annual binned level 3b SeaWiFS images of normalized water-leaving radiance at 555 nm (nLw_{555}) were obtained from the NASA Ocean Color Web Facility (<http://oceancolor.gsfc.nasa.gov/>) for the Great Lakes region from January 1998 to December 2005. These level 3b products are atmospherically corrected radiances combined into 4km spatial bins. Water-leaving radiance data were converted into a water clarity index using a simple empirical relationship and used to study temporal and spatial variations in water clarity over the Great Lakes (see section 4.1). Daily binned level 3b data files were obtained coincident with in situ observations of water clarity for validation purposes.

CZCS

CZCS L3b monthly binned images were obtained from the NASA Ocean Color Web Facility for Band-3 radiance at 550 nm for the period January 1979 to December 1985. Water-leaving radiance data were converted into a water clarity index using a simple empirical relationship and used to study temporal and spatial variations in water clarity over the Great Lakes in conjunction with SeaWiFS imagery above (see section 4.1). Daily binned level 3b data files were obtained coincident with in situ observations of water clarity for validation purposes.

MERIS

MERIS L2 data coincident with research cruises on Lakes Erie and Ontario were ordered from ESA's EOLI-SA catalogue and ordering service and processed using ESA/Brockmann Consult's BEAM VISAT toolbox for image analysis and processing. Water-leaving reflectance at the wavelengths 412.5, 442.5, 490, 510, 560, 620, 665, 681.25, 705, and

753.75, along with the MERIS standard water quality products (Algal 1, Algal 2, Yellow substance and Total suspended matter) were extracted for each station location.

LANDSAT

An archive of Landsat 5 and 7 TM images of the Laurentian Great Lakes has been accumulated over the last 20 years at NWRI. A total of forty-eight clear-sky scenes of Lake Ontario are present in the archive. The 30 metre resolution of the thematic mapper is able to detect small plumes entering the lake from its tributaries. The 3 broad bands in the visible spectrum can be related to the total particulate loadings within the plumes. Unfortunately the 16 day interval between overpasses, and the coincidence of cloud cover with storm events greatly limits the ability of LANDSAT to observe such events.

3.2 IMAGE ARCHIVE

All imagery has been stored to create a substantial archive of satellite aquatic colour imagery for the Great Lakes region (Table 5).

Table 5: Aquatic colour satellite image archive for the Great Lakes region

Sensor	Daily	Biweekly	Monthly	Annual	Current Processing
MODIS	✓ 2005- present	✓ 2005- present	✓ 2005- present	✓ 2005- present	Yes, ongoing, backdating to 2002 Proposed operational processing
SeaWiFS	✓ Selected dates	✗	✓ 1997- 2005	✓ 1997- 2005	Yes, ongoing, completing archive to present
CZCS	✓ Selected dates	✗	✓ 1979- 1986	✓ 1979- 1986	No Used for historical time-series analysis
MERIS	✓ Selected dates	✗	✗	✗	No Analysed for model development & validation
Landsat	✓ Clear images 1985-'03	✗	✗	✗	No Event-specific observations

4 WATER QUALITY REMOTE SENSING; MODELLING, VALIDATION & APPLICATIONS

4.1 A SIMPLE ASSESSMENT OF WATER CLARITY CHANGE IN THE GREAT LAKES

Water-leaving radiance in the green portion of the visible spectrum (~550 nm) is often treated as an indicator of general turbidity; scattering caused by organic and inorganic particles in suspension lead to elevations in the measured water-leaving radiance. Whilst it is not possible to distinguish the different types of scattering materials from a single band reflectance, with prior knowledge of the Great Lakes system it is possible to infer the timing and location of bright-water episodes such as intense phytoplankton blooms, suspended sediments and whiting events. Binding et al. (2007) presented water-leaving radiance data from both the CZCS (in operation from 1978 until 1986) and SeaWiFS (1997 to present) sensors that could be interpreted in terms of changes in water clarity of the Great Lakes aquatic system.

Figure 8a and 8b present CZCS nLw_{550} and SeaWiFS nLw_{555} for the Great Lakes region averaged over the periods 1979-1985 and 1998-2005 respectively. The large geographical variation in water-leaving radiance is noticeable, with Lake Erie exhibiting the highest radiance and Lake Superior the lowest. Regions of water clarity change may be inferred from these images by simple subtraction of the means (Figure 8c). From figure 8c it can be seen that lakes Michigan and Huron appear to have been brighter during the 1979-1985 period than the 1998-2005 period although several shallow near-shore areas such as Saginaw Bay and Lake St. Clair exhibit significantly brighter waters in more recent years. Lake Superior has shown the least change in mean brightness between the two time periods whereas Lake Ontario in its entirety exhibits significantly lower image brightness during the SeaWiFS mission than the CZCS mission two decades prior. Imagery of Lake Erie suggests more complex change with the central and western basins appearing much brighter in recent years whereas the eastern basin waters are less bright than during the CZCS mission years.

Temporal variability was assessed in more detail from time-series plots of monthly lake-averaged water-leaving radiance (see Binding et al. 2007 for full study), showing seasonal and inter-annual variability in brightness signals that may be related to periods of phytoplankton blooms, mineral sediment suspension, and whiting events. Few data sets of in situ optical properties exist dating as far back as the 1970s, making validation of such a long term data set difficult. However, one consistent measurement made by Environment Canada over the years is water transparency: over the period of interest 7780 Secchi disk observations were made within Lakes Erie and Ontario during routine research and surveillance cruises. Utilizing these datasets, a simple method of estimating Secchi depths from satellite measured aquatic colour was derived and used in the retrospective analysis of water clarity conditions of Lakes Ontario and Erie.

CZCS and SeaWiFS imagery was obtained in the form of L3b daily composites and clear-image radiances coincident with in situ sampling dates were extracted. Strong empirical relationships between Secchi disk depths and both CZCS and SeaWiFS water-leaving radiance were evident (Figure 9, Table 6). These relationships were subsequently applied to the archived monthly composite images in order to determine long term trends in water clarity for Lakes Erie and Ontario.

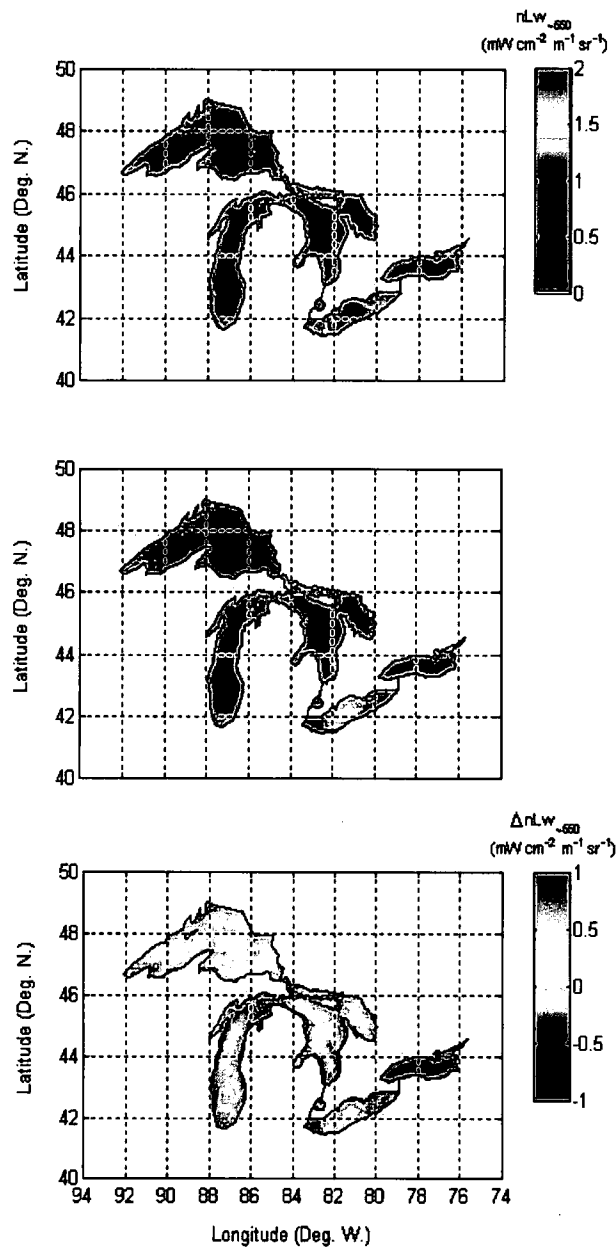


Figure 8: (a) Average CZCS nLw_{550} for the period 1979-1985, (b) average SeaWiFS nLw_{550} for the period 1998-2005 and (c) difference between the two images.

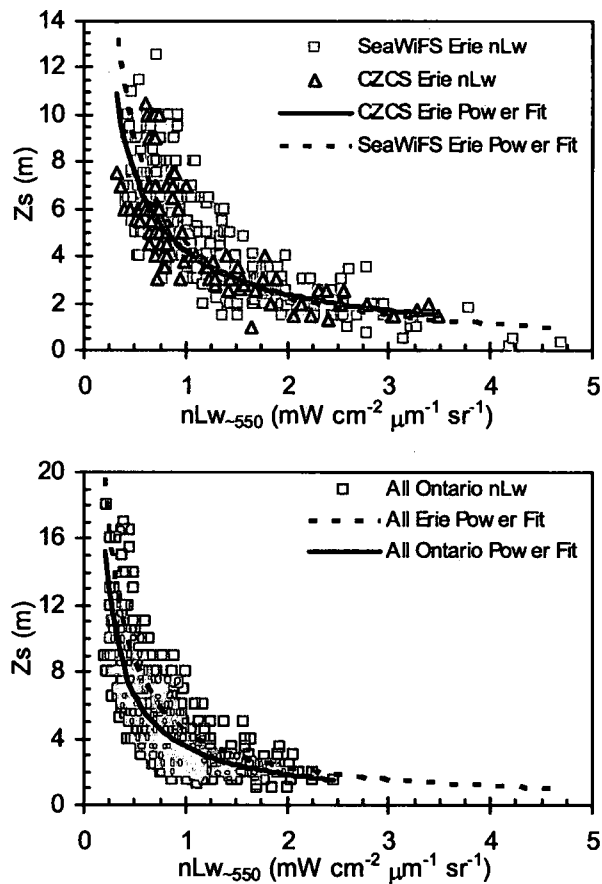


Figure 9: Secchi disk depth (Z_s) against coincident SeaWiFS nLW_{555} and CZCS nLW_{550} during surveys on (a) Lake Erie and (b) Lake Ontario. Least square regression equations of the form $Z_s = \alpha nLW^\beta$ are presented in table 1.

Table 6: Least square regression coefficients of the form $Z_s = \alpha nLW^\beta$ for data sets of in situ Secchi disk depth (Z_s) and coincident satellite nLW_{550}

Data-set	α	β	R^2	n	p
Erie SeaWiFS	4.518	-0.991	0.72	306	<0.05
Erie CZCS	4.211	-0.821	0.70	94	<0.05
All Erie	4.443	-0.949	0.71	400	<0.05
All Ontario	3.505	-0.923	0.65	420	<0.05

Figures 10a and 10b present the average Secchi depth over Lake Erie for the periods 1979-1985 and 1998-2005 respectively. Lake-wide Secchi depths ranged from 2 to 4.5 m and 1.5 to >6 m for the CZCS and SeaWiFS missions respectively, with the geographic distribution varying considerably between the two periods. Secchi depths of 4 m and greater, whilst quite widespread in the central and eastern basin during 1979-1985, are confined strictly to the

eastern basin during the 1998-2005 period. Figure 10c shows the change in Zs between the two periods and confirms the relative increase in water clarity of up to and exceeding 2 m throughout the eastern basin. In contrast, the central and western basins have undergone a period of decreasing water clarity, with average reductions in Zs of 1-2 m.

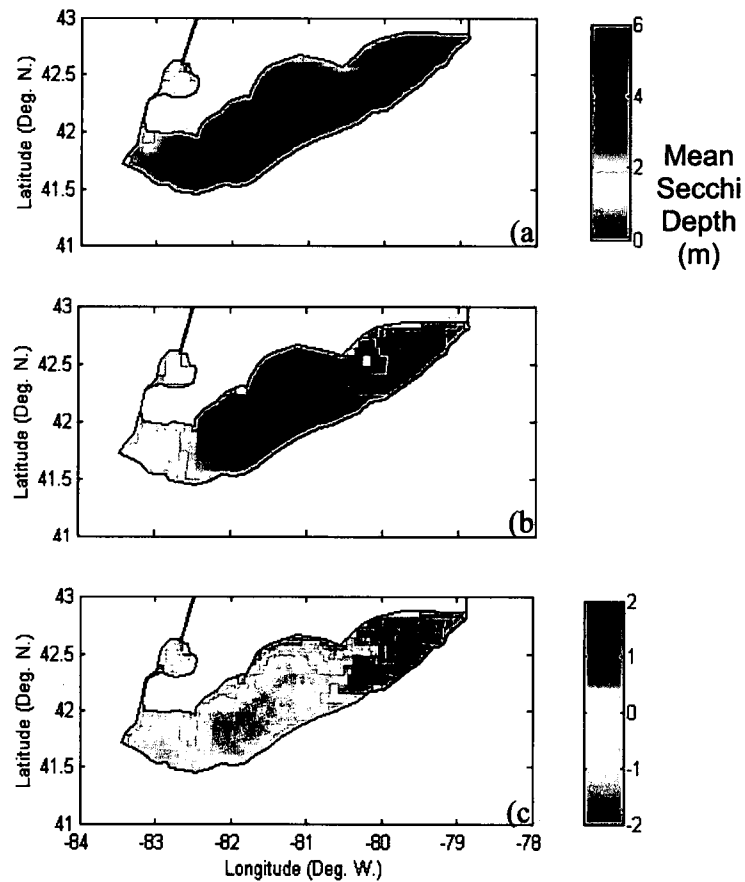


Figure 10: Average Lake Erie Secchi disk depth (meters) for the periods (a) 1979-1985 and (b) 1998-2005 and (c) change in Secchi depth between the two periods.

Average Secchi depths over Lake Ontario as estimated from CZCS and SeaWiFS imagery for the periods 1979-1985 and 1998-2005 respectively are presented in figures 11a and 11b. Secchi depths are largely uniform across the lake at around 3 - 4 m for the 1979-1985 period and increase noticeably to 6-8 m by the 1998-2005 period. Figure 11c confirms that the entire lake appears to have undergone significant improvements in water clarity, with a lake-wide increase in Secchi depth of between 2 and >4 m.

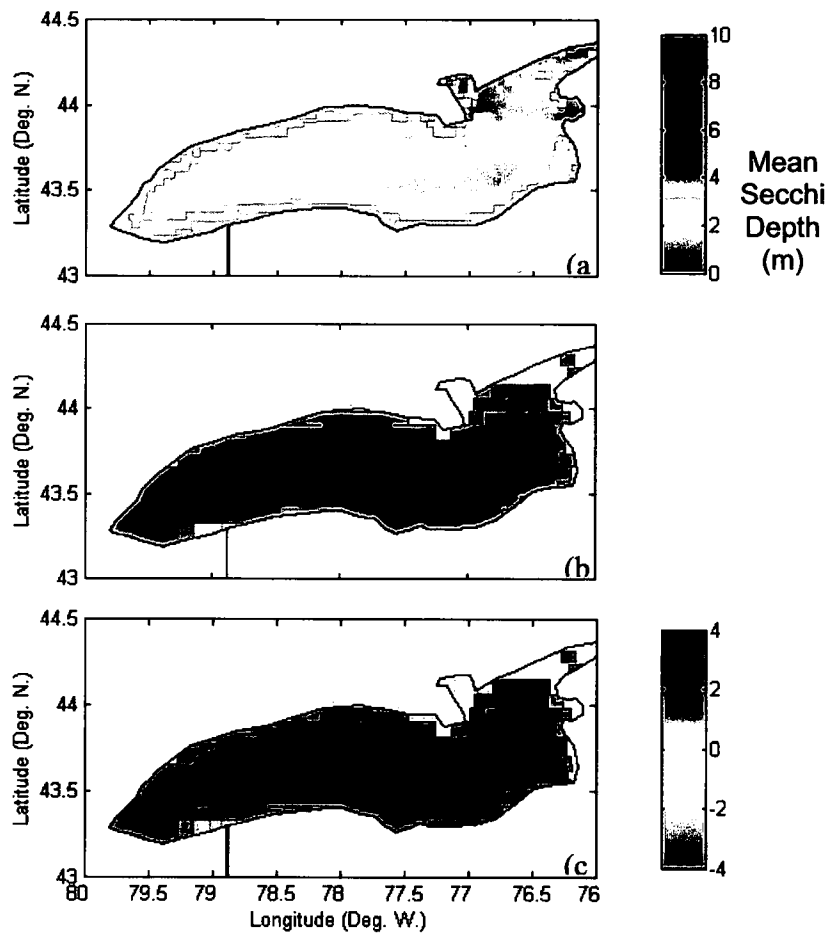


Figure 11: Average Lake Ontario Secchi disk depth (meters) for the periods (a) 1979-1985 and (b) 1998-2005 and (c) change in Secchi depth between the two periods.

Binding et al. (2007) presents further details on monthly water clarity changes in both lakes, documenting the effects of seasonal processes on water clarity. The trends identified are in agreement with long term ground-based studies of water quality change reported by Barbiero & Tuchman (2004) and Makarewicz *et al.* (1999) and may be linked to the combined effects of a decrease in productivity associated with lower nutrient loadings to the lakes, particulate removal through mussel filter-feeding and a decrease in the intensity and frequency of whiting events brought about by calcium uptake by mussel populations. Given the varying environmental conditions and inherent subjectivity with which Secchi disk measurements are made the relationships determined in this study are surprisingly robust, with average errors of less than 25%. These errors are consistent with NASA's goal of retrieving water quality information (primarily chlorophyll) from ocean colour sensors with an accuracy of 35% (McClain *et al.*, 2004).

4.2 INVERSE MODELLING OF MODIS RED/NIR WAVEBANDS FOR THE MONITORING OF SUSPENDED PARTICULATES

Techniques for determining concentrations of suspended particulate matter (SPM) from space have historically been based either on spectral changes (through reflectance ratios or full colour spectrum analysis) or brightness (through single-band reflectance). The choice of approach and wavelength selection depends primarily on the optical complexity of the water (specifically to what degree SPM dominates the optical signal) and the concentration range of SPM present. The success of algorithms based on short-wavelength colour ratios has, for the most part, been restricted to regions where mineral sediments are likely to dominate the optical signal such as the Bay of Fundy (Amos and Topliss, 1985; Topliss, 1986) and the Humber Estuary (Robinson *et al.*, 1998). Elsewhere, large errors may be incurred due to the presence of co-varying in-water constituents such as chlorophyll and coloured dissolved organic matter (CDOM) (Bukata *et al.* 1995; Novo *et al.*, 1989; Binding *et al.*, 2003). Utilising wavelengths in the red/near-infra-red portion of the spectrum, where the influence of CDOM and Chlorophyll on the optical properties is greatly reduced, may therefore offer improved accuracy in determinations of SPM concentrations from satellite observations of aquatic colour. This study explores the use of MODIS wavebands in the red/near-infra-red for estimating SPM concentrations in the turbid, optically complex waters of Lake Erie. The complete study is presented in Binding *et al.* (2008).

MODIS wavebands centred at 667 nm and greater were considered for deriving SPM concentrations in Lake Erie. A preliminary assessment was based on the strength of correlations between the spectral water-leaving radiance and the in situ measured SPM concentrations. Table 7 presents the correlation coefficients between SPM concentrations and both band ratios and single band water-leaving radiance for each of the MODIS bands centred at 667, 678, 748 and 869 nm. The ratio of the two bands centred at 667 and 678 nm, aligned with chlorophyll-a absorption and fluorescence respectively, resulted in the weakest correlation with [SPM] whereas single band water-leaving radiance at 748 and 869 nm showed the strongest correlations with [SPM]. Although bands 748 and 869 show equally strong correlations with [SPM], it is expected that 748 will be more sensitive to lower concentrations, with 869 more suitable to extremely turbid waters. From this preliminary analysis it is therefore suggested that nlw748 may be the best waveband for the determination of SPM concentrations in Lake Erie from MODIS data and therefore it is this waveband that will be explored further in terms of inverse modelling procedures.

<i>nLw667</i>	0.69			
<i>nLw678</i>	0.09	0.67		
<i>nLw748</i>	0.78	0.73	0.95	
<i>nLw869</i>	0.78	0.73	0.79	0.95
R_1/R_2	<i>nLw667</i>	<i>nLw678</i>	<i>nLw748</i>	<i>nLw869</i>

Table 7: Correlation coefficients between MODIS red and NIR water-leaving reflectance ratios (R_1/R_2) and SPM concentrations. Shaded regions indicate correlations with reflectance at a single wavelength.

Modelling SPM from MODIS nLw748

Inverse modelling of the remotely sensed signal to retrieve a water quality product such as SPM first requires the conversion of the water-leaving radiance into the inherent optical properties of the water body under consideration. The normalized water leaving radiance, nLw, can be related to the volume reflectance, R, by:

$$nLw = F_0 \frac{(1-\rho)(1-\bar{\rho}) R}{n^2(1-\bar{r}R) Q} \quad (2)$$

where F_0 is the extraterrestrial solar spectral irradiance at mean earth-sun distance, n is the refractive index of water, ρ is the Fresnel reflectance at the air-water interface for incident downward radiance, $\bar{\rho}$ the Fresnel reflectance at the air-water interface for the downward sky irradiance. The ratio $\frac{(1-\rho)(1-\bar{\rho})}{n^2}$ combines the effects of reflection and refraction at the air-water interface and can be approximated to 0.54 (Austin, 1974; Morel & Gentili, 1993, 1996). The term $(1-\bar{r}R)$ describes the fraction of the upwelling irradiance that is reflected downwards at the water-air interface and contributes to the in-water downwelling irradiance where \bar{r} , the mean water-air Fresnel reflectance, is approximately 0.48 (Morel & Mueller, 2003). The Q function takes on a value of π for an isotropic radiance distribution.

The volume reflectance is commonly related to the backscattering and absorption coefficients by a factor f , which here is given the value 0.319 after Jerome et al. (1988), enabling the backscattering to absorption ratio (b_b/a) to be estimated from MODIS nLw748 (equation 3).

$$R = f \frac{b_b}{a} = \frac{nLw}{0.54F_0 / \pi + 0.48nLw} \quad (3)$$

This procedure was carried out for daily MODIS imagery of nLw748 from January 2005 December 2007. Image data coincident with in situ observations during the 2004/2005 field season were extracted. In situ $b/a(748)$ determined according to section 2.2 were compared with MODIS-derived $b_b/a(748)$ using least squares regression. With an intercept not significantly different from zero, the regression was forced through the origin, producing equation 4.

$$b/a_{(in\ situ)} = 51.162(+/- 1.736)b_b/a_{(MODIS)} \quad (R^2 = 0.93, n=67) \quad (4)$$

The slope of 51.162 produces an estimated value of b_b/b of 0.0195 which is within the documented range of b_b/b for turbid waters and in surprising agreement with the 0.019 frequently adopted after Petzold (1972). Such a strong agreement suggests that the image data and the processing procedures can be deemed reasonable for this dataset.

At 748nm, scattering and absorption can be attributed to particulate matter and water alone (equation 5). By combining equations 3 and 5, and using the coefficients in Table 8, it is possible to determine the concentration of total suspended particulate matter, SPM.

$$\frac{b_b}{a}(748) = \frac{b_{bw} + b_{SPM} b_b/b[SPM]}{a_w} \quad (5)$$

The mass-specific scattering coefficient for suspended particulates (b^*_{SPM}) was determined according to section 2.2.2 and assumed to be spectrally neutral across the wavelength selection under study here, therefore coefficients determined at 660 nm^{-1} were used for modelling of all red/NIR wavelengths. Scattering coefficients obtained during a separate study of Lake Ontario waters using a Wetlabs AC9 produced an average scattering ratio $b_{715}:b_{660}$ of 0.985 with a standard deviation of 0.05, therefore suggesting that this assumption may be valid. Particulate and dissolved absorption at 748 nm was assumed to be negligible and therefore total absorption at this wavelength attributed to water alone. The modelling procedures outlined here were applied to daily MODIS imagery and SPM concentrations derived. MODIS-derived SPM concentrations at those pixels coincident with cruise observations were compared and showed a strong 1:1 agreement (Figure 12, Equation 6), with an rms error in predicted spm of 40% of the mean, or 1.20 g m^{-3} .

$$[SPM]_{MODIS} = 1.033[SPM]_{Meas} - 0.1489 \quad (R^2 = 0.90, n=70) \quad (6)$$

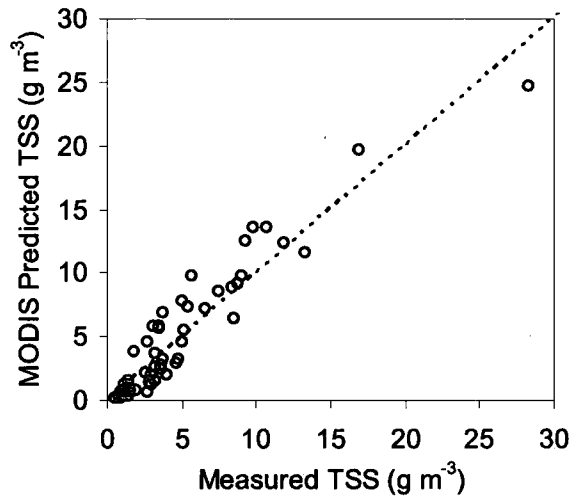


Figure 12: Measured TSM concentrations versus those modelled from MODIS nLw748.

Table 8: Model parameters

Function	Value	Source
F_0	128.123	OCDPG*
\bar{r}	0.48	Morel & Mueller (2003)
Q	πsr	Assuming isotropic radiance field
f	0.319	Jerome <i>et al.</i> (1988)**
a_w	2.8 m^{-1}	OCDPG*
b_b/b	0.019	Petzold (1972)
b_bW	0.00027 m^{-1}	OCDPG*
b^*_{SPM}	0.554 g m^{-2}	Derived in this study

* NASA/GSFC's Ocean Color Discipline Processing Group (OCDPG) computed spectral response functions and bandpass averaged quantities were used during image processing and modelling procedures. (http://oceancolor.gsfc.nasa.gov/DOCS/RSR_tables.html).

** For vertically incident radiance under clear skies.

Total water column suspended loads

Within environmental monitoring it is often pertinent to know the total mass of SPM suspended within the water column, for example when contaminated sediment is re-suspended following a storm event, or total sediment transport budgets are required. It would therefore be of significant practical use if estimates of total water column SPM loads can be estimated. The rapid in-water attenuation of radiation at 748 nm means that the water-leaving radiance originates from a very small surface layer of water; for SPM concentrations up to 30 g m^{-3} that depth (estimated as $1/K_d$) may be as little as 30 cm. As a result, satellite determinations of SPM utilising this wavelength will estimate only surface concentrations and distributions.

The nature of Lake Erie (being shallow and exposed to strong wind-driven mixing) results in predominantly mixed water column conditions, resulting in a consistent relationship between attenuation averaged over depth, c_d , and that measured at the surface, c_s , (Equation 7). The attenuation coefficient, c , in these waters is determined almost entirely by the concentration of SPM (Equation 8), therefore combining the MODIS-estimated surface concentrations of SPM, equations 7 and 8, and a detailed bathymetric grid of Lake Erie enables lake-wide total water column suspended loads to be estimated.

$$c_d = 0.907c_s + 0.15 \quad (R^2 = 0.89, n=594) \quad (7)$$

$$c = 0.523[\text{SPM}] + 0.50 \quad (R^2 = 0.94, n=90) \quad (8)$$

The total sediment load held in suspension is governed by the available turbulent kinetic energy which in Lake Erie is primarily wind generated. The power in the wind is proportional to the wind speed cubed and therefore a close agreement between suspended sediment concentrations and W^3 should be expected. Figure 13 shows a time-series of lake-wide average total water column SPM loads estimated from the biweekly MODIS composite images of nLw748 as well as an estimate of W^3 . Wind speed data was obtained from the National Oceanic and Atmospheric Administration's National Data Buoy Center. Biweekly lake-wide wind speeds were calculated from the average wind speeds recorded at four buoys in Lake Erie (NDBC 45005, Canadian buoys 45132 and 45142 and GLERL buoy THLO1). Figure 13 shows a clear dependence of water column SPM on wind speed (there is a positive correlation between SPM and W^3 with $R = 0.85$), identifying several strong resuspension events during winter storm seasons. Imagery can be used to quantify the total lake-wide suspended sediment load following a specific wind event. For example, for the period 3-16 December 2006, when the average wind speed over Lake Erie was 8.9 m s^{-1} (reaching a maximum of 14.4 m s^{-1} on December 9), the average mass of sediment held in suspension at any one time was 5.8 million metric tonnes, more than four times the average over the year of 1.3 million tonnes. The total mass of sediment held in suspension during this single wind event is just under half the 14.9 million metric tonnes of fine-grained sediments estimated by Kemp et al. (1977) to be entering the lake from external sources on an annual basis.

Figure 14 shows the resulting monthly composite total water column SPM maps for Lake Erie from January 2003 to December 2007 as derived from the inverse modeling of MODIS nLw748. Imagery identifies a strong seasonal cycle in SPM concentrations, with significantly elevated concentrations between November and February each year. Imagery highlights the western basin as an area of high suspended loads but also near-shore areas on the north and south shores of the central basin associated with regions of strong shoreline erosion.

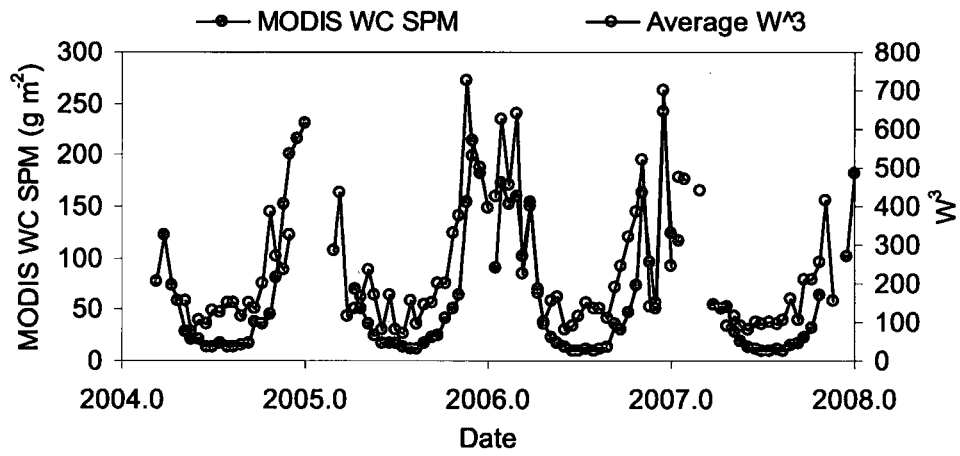
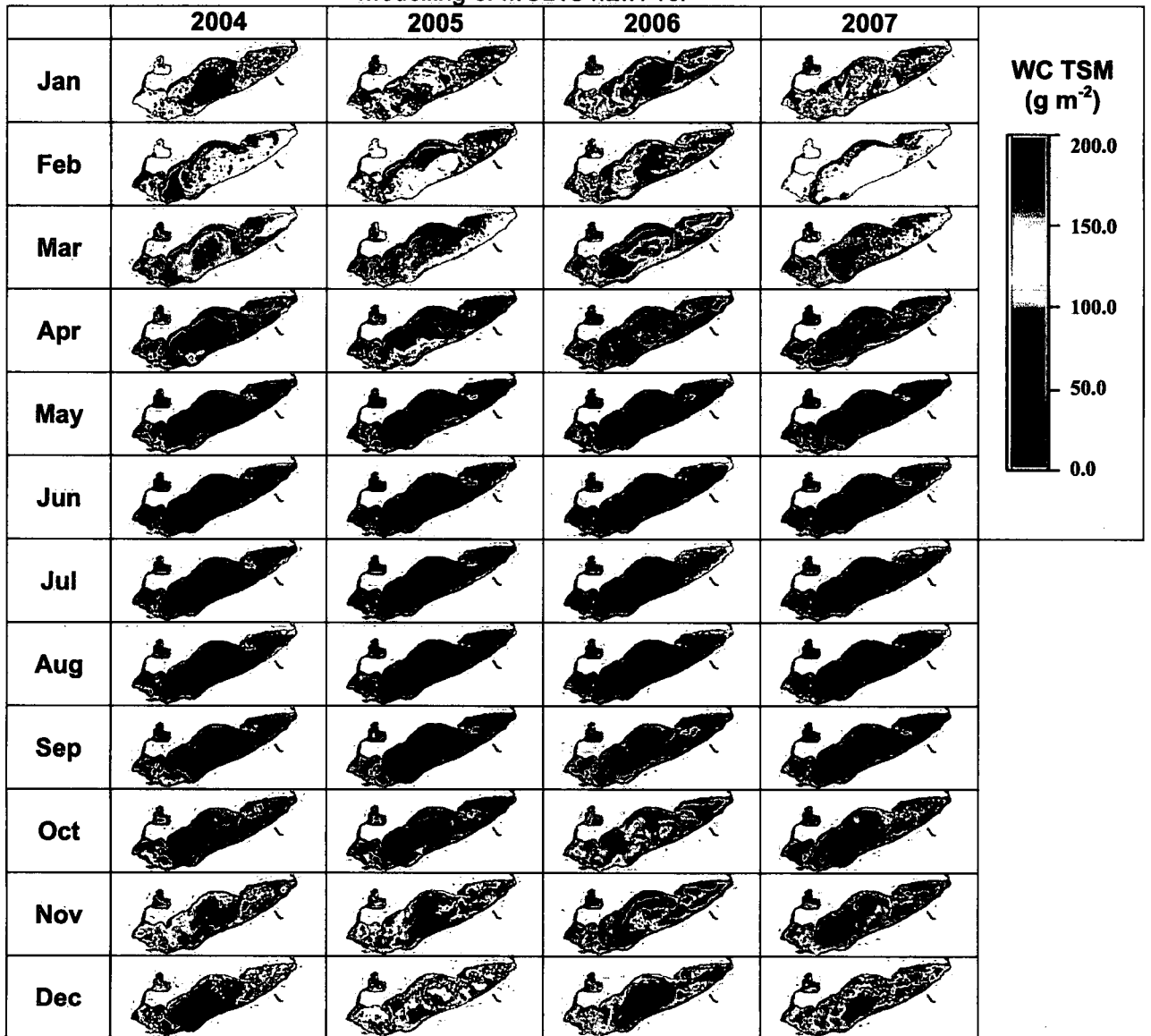


Figure 13: MODIS-estimated biweekly lake-wide mean Water Column (WC) SPM concentrations, and W^3 (wind speed cubed) obtained from Lake Erie buoyed weather stations.

Figure 14: Monthly mean distribution of total water column SPM (g m^{-2}) derived from inverse modelling of MODIS nLw748.



4.3 INVERSE MODELLING OF MODIS RED/NIR WAVEBANDS FOR THE MONITORING OF ALGAL BLOOMS

Aquatic colour algorithms for estimating concentrations of chlorophyll-a traditionally rely on the colour changes brought about by the absorption by chlorophyll-bearing biota of light in the blue part of the visible spectrum, resulting in the typical water colour changes from blue oligotrophic waters to green eutrophic waters. These algorithms, based on blue to green radiance ratios, work well in Case-1 waters (mostly open ocean, where phytoplankton dominate the optical signal) but fail in Case-2 waters where mineral particulates, dissolved organic matter and other optically active constituents create a level of optical complexity which renders these simple algorithms ineffective. The waters of the lower Great Lakes fall within this Case-2 water classification thereby necessitating alternative methods for the retrieval of chlorophyll concentrations from satellite-measured aquatic colour. The potential for using the red/NIR wavebands of MODIS for estimating chlorophyll concentrations in the Great Lakes is explored here. The method relies on the chlorophyll absorption peak at ~670 nm, a portion of the spectrum where absorption by other material can be assumed negligible and scattering may be assumed spectrally invariant, at least over short wavelength intervals. The following sections describe the modeling procedures in more detail.

Here we adopt two MODIS wavebands to model chlorophyll absorption; 667 nm, coinciding with the peak of chlorophyll absorption, and 748 nm, where chlorophyll absorption can be assumed to be negligible. Assuming absorption at 748 nm can be attributed to water alone and that at 667 nm to phytoplankton, mineral sediments and water (CDOM absorption is assumed to be negligible at both wavelengths), then the optical properties can be related to the ratio R_{667}/R_{748} according to equation 9.

$$\frac{R_{667}}{R_{748}} = \frac{f[b_{\text{bSPM}}/a_{\text{W}} + a_{\text{MSS}} + a_{\text{C}}]_{667}}{f[b_{\text{bSPM}}/a_{\text{W}} + a_{\text{MSS}}]_{748}} \quad (9)$$

In equation 9 b_{bSPM} is the total backscattering by suspended particulates, a_{MSS} the absorption by mineral sediments and the factor f , which here is given the value 0.319 after Jerome et al. (1988). Assuming spectrally invariant b_{bSPM} , a_{MSS} and f , equation 9 simplifies to equation 10, relating the reflectance ratio to the absorption properties of chlorophyll and water alone, from which the concentration of chlorophyll can be obtained given a realistic value for the absorption cross-section for algal matter (equation 11).

$$\frac{R_{667}}{R_{748}} = \frac{a_{\text{W}748}}{[a_{\text{W}} + a_{\text{C}}]_{667}} \quad (10)$$

$$a_{\text{C}667} = [\text{CHL}]a_{\text{C}667} \quad (11)$$

Whilst it is known that the absorption properties of phytoplankton vary with cell size and species, a simple assumption that $a^*C=0.025 \text{ m}^{-2} \text{ mg}^{-1}$ as shown in section 2.2.1 and several other studies appears to work well here as a first approximation (Figure 15).

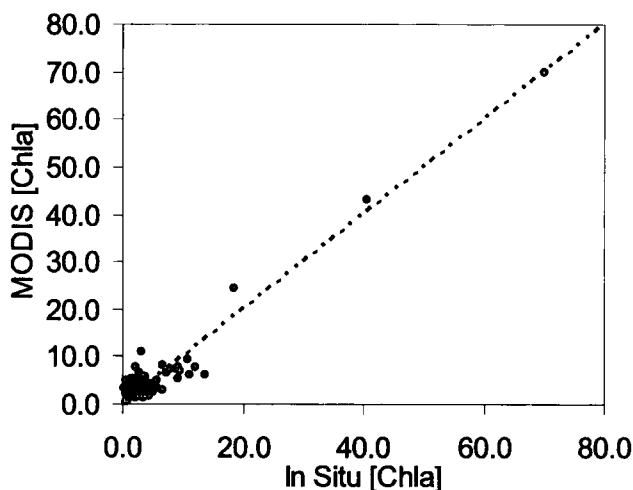


*Figure 15: Agreement between in situ [chla] and that predicted from MODIS through inverse modeling assuming a^*C_{667} of 0.025.*

These modeling procedures were applied to monthly composite MODIS imagery of the Great Lakes for the year 2004 in order to map algal blooms. A threshold chlorophyll concentration of 15 mg m^{-3} was used to flag a significant algal bloom occurrence as shown in figure 16. This imagery shows clear spring and fall algal blooms in the near-shore areas of the Great Lakes, but also identifies isolated mid-lake pixels as high chlorophyll particularly in the winter months. It is suggested that these pixels are in fact contaminated pixels on cloud or ice edges that have elevated radiance in the red and thus resulting in falsely elevated chlorophyll estimations.

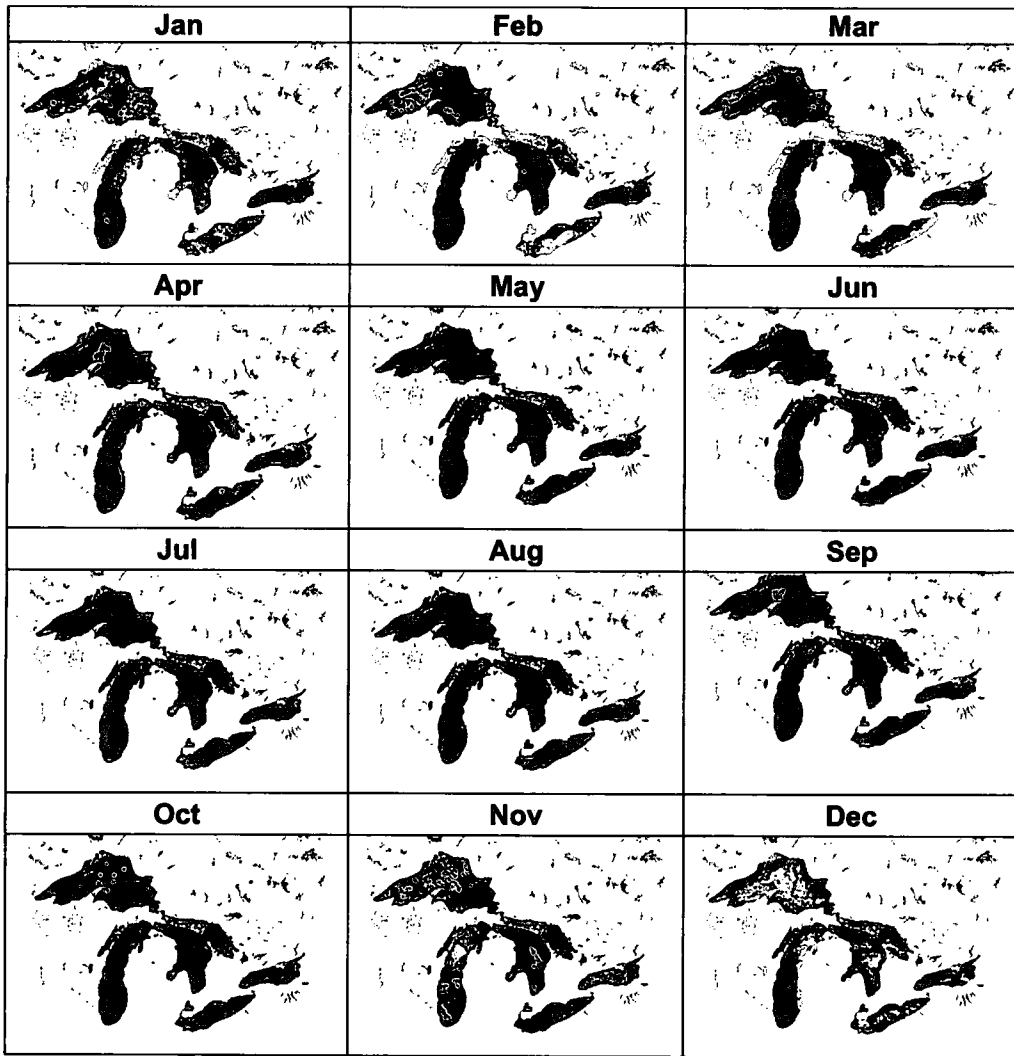


Figure 16: Algal bloom flag before correction for erroneous cloud/ice edge pixels. Red pixels indicating inferred chlorophyll concentrations greater than 15 mg m^{-3} .

Extracting the full radiance spectrum for these pixels and comparing them with those of typical chlorophyll dominated waters (Figure 17) identifies distinct differences in the spectral water-leaving radiance, showing that for those erroneously flagged pixels the typical reduction in blue radiance associated with the strong absorption by chlorophyll is not present. By adding a conditional statement to the model that required nLw_{531} to be less than nLw_{551} in these chlorophyll rich waters, eliminates the majority of these suspect data (Figures 18-20). The corrected data results in realistic spatial and temporal distributions of algal blooms in the Great Lakes, reproducing the spring and autumn bloom periods in regions known to be prone to excessive algal growth such as Sandusky Bay, Saginaw Bay, Green Bay and several other near-shore zones.

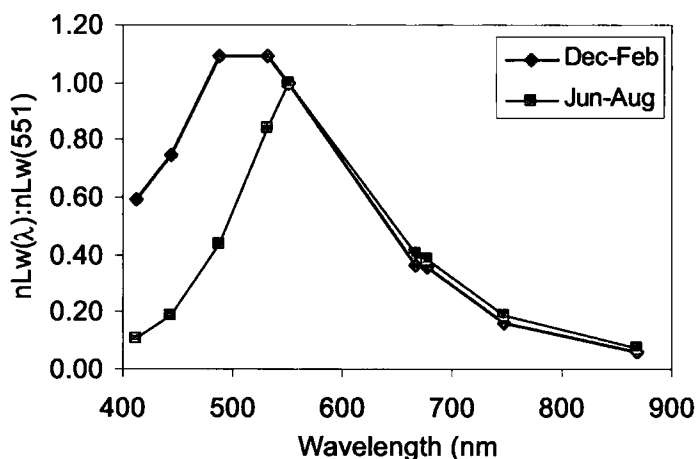


Figure 17: Normalized spectral water-leaving radiance for typical algal dominated waters flagged as chlorophyll $> 15 \text{ mg m}^{-3}$ (pink) and those erroneous pixels flagged in winter (blue).

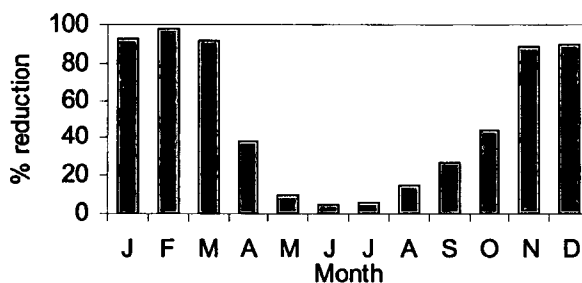


Figure 18: Percentage reduction in pixels flagged as having chlorophyll concentration greater than 15 mg m^{-3} following $nLw_{531} < nLw_{551}$ condition.

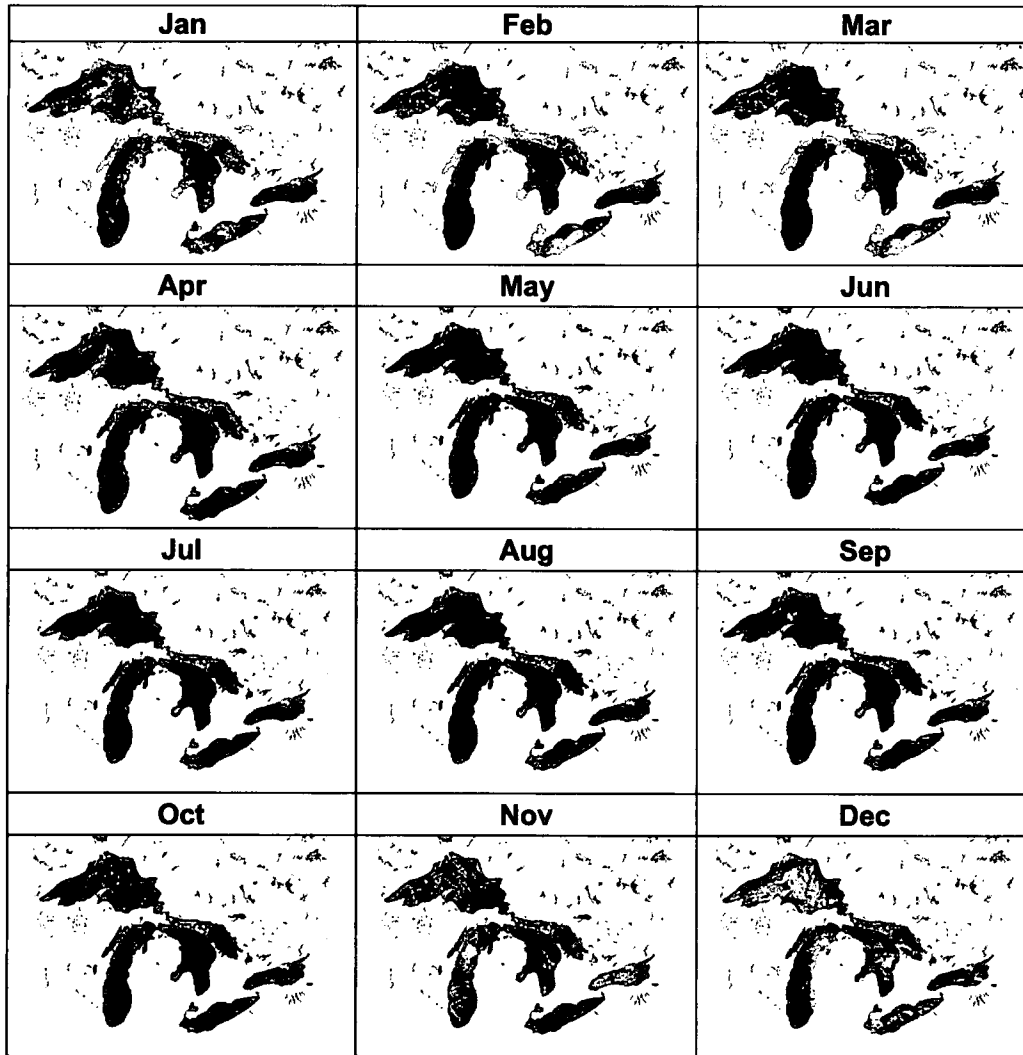


Figure 19: Algal bloom flag after correction for erroneous cloud/ice edge pixels. Red pixels indicating inferred chlorophyll concentrations greater than 15 mg m^{-3} .

5 RELATING WATER QUALITY TO LAND USE IN THE GREAT LAKES WATERSHED - Lake Ontario Watershed Loadings

In this section of the study, loadings from Lake Ontario watersheds to Lake Ontario for a number of water quality parameters of concern, including total phosphorus (TP), nitrate (NO₃), nitrite (NO₂), total nitrogen (TN) as well as total suspended solids (TSS) have been determined for the period 1980-2005.

The objectives were to:

- Determine Event Mean Concentrations coupled with runoff volumes as a first approximation of watershed loads across the region;
- Use unit area loads from PLUARG and other studies to estimate unit area loads (kg/ha) for nutrients on a watershed and sub-watershed basis;
- Run event water quality model (AGNPS) to estimate peak loads for major storm events;
- Compare wet weather flow and other modelling studies with available concentrations and loads;
- Where opportunities exist, use measured flow and stream chemistry data (MOE and enhanced PWQMN) data to calculate observed loads and calibrate models;

The study area includes all watersheds from Niagara in the west to Prince Edward County in the east, as shown in Figure 20. Those tributaries for which sufficient data was available to calculate loadings are listed in Table 1.1 of the Appendix 1.

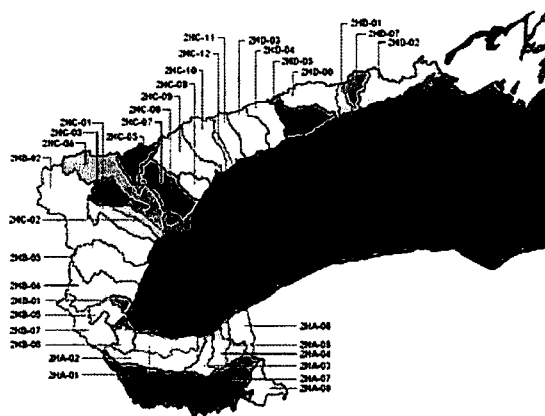


Figure 20: Lake Ontario Quaternary watersheds

5.1 UNIT AREA LOADS METHOD

The unit loads method requires land use GIS layers for the study watersheds. The default unit area loads used for this study are shown in Table 9 They were determined from a literature review of earlier studies in Canada (International Reference Group on Great Lakes Pollution from Land Use Activities , Task Group C, 1978; Ostrey and Tseng, 1981; Winter et al, 2002, Stantec and Aquafor Beech, 2003; Aquafor Beech and Monitario Technical Services, 2005) and the US (Dodd et al. 1992; Corsi et al., 1997; PLUARG, USGS, etc.). Values determined in these studies are listed in Tables 10 and 11. Unfortunately, none of the studies determined unit area coefficients for all of the land use classifications or for all of the study parameters.

Table 9: Unit Area load coefficients for various land uses.

Land Use	TP Export (kg/ha/yr)	TN Export (kg/ha/yr)	TSS Export (kg/ha/yr)
Conifer Swamp	0.1	2.2	100
Coniferous plantation	0.1	2.2	100
Cropland	0.8	8.0	240
Deciduous swamp	0.1	2.2	100
Dense coniferous forest	0.1	2.2	100
Dense deciduous forest	0.1	2.2	100
Freshwater coastal/inland marsh	0.65	12.4	150
Mixed forest, mainly coniferous	0.1	2.2	100
Mixed forest, mainly deciduous	0.1	2.2	100
Open fen	0.65	12.4	150
Pasture and abandoned fields	0.5	5.0	210
Settlement and developed land	1.2	9.0	370
Sparse deciduous forest	0.5	2.2	210
Water	0.65	12.4	150
Bedrock	0	0	0

Table 10: Winter et al. 2002 unit area load coefficients

	Agricultural	Forested	Urban
Total Phosphorus (kg/ha/yr)	0.11-.27	0.06-.07	0.65
Total Nitrogen (kg/ha/yr)	2-12	1.2 – 3.9	5 - 16

Table 11: PLUARG 1975-77 average unit area loads

Watershed	TSS (kg/ha/yr)	TP (kg/ha/yr)	TN (kg/ha/yr)
Bowmanville Cr.	55.3	0.13	3.5
20 Mile Cr.	331	1.46	14.0
Humber River	164	0.44	8.4

The land use data for all of the watersheds was derived from Provincial Land Cover 1998, County Official Plans, and AgCan: 2003 Landuse Coverage. The land cover map used is shown in Figure 2.1 of Appendix 2. They were determined as percentage coverage and entered into a spreadsheet to calculate individual loads and summed as shown in Figure 21 for Bronte Creek.

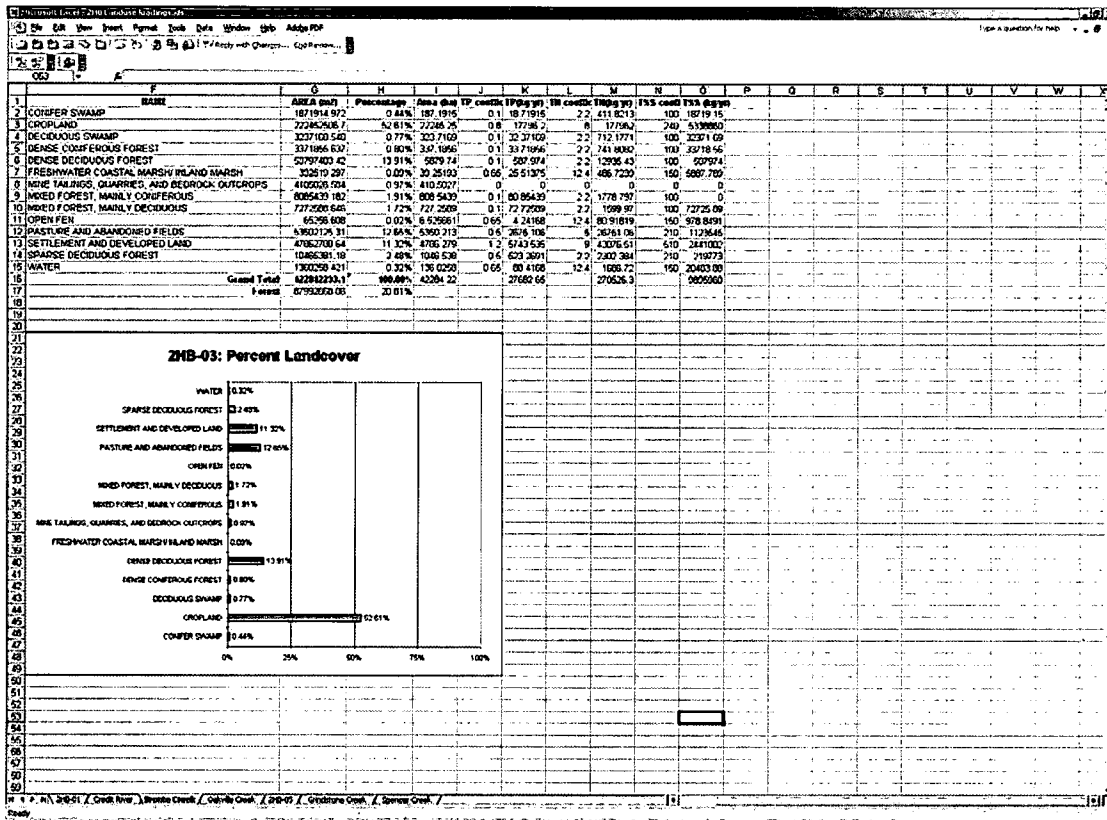


Figure 21: Example unit area load calculations for Bronte Creek

5.2 EVENT MEAN CONCENTRATIONS METHOD

The event mean concentration method is used based upon years of measured wet and dry weather stream concentrations and flows for nutrients and TSS. Typically the determination of wet versus dry is done by examining the hydrograph from the nearest flow sampling location. A review of the literature was used to compile EMC wet and dry values to be used for the various types of watersheds in the study area (Aquafor Beech, 2005; MOE/EC, 1999; City of Toronto, 2000; Stantec/Aquafor Beech, 2003; and TRCA, 2001). Where values were determined for specific watersheds they were applied directly to those watersheds. Where no directly determined values had been determined, values from adjacent watersheds were used if the land use, soils and slopes were similar. As this study is concerned with determining drinking water protection zones, which would typically be impacted by storm events, the focus of the EMC results will be more on the wet weather loads.

The event mean concentration loads were determined for the years 1980, 1991, 1999, 2003, 2004 and 2005 for daily, monthly and annual time steps. Flows were obtained from the Water Survey of Canada gauging station records available from the archived hydrometric data web site (<http://www.wsc.ec.gc.ca/hydat/H2O>). The gauging stations are typically not located at the stream mouths of Lake Ontario. Consequently, the flows were multiplied by a correction factor to represent the entire drainage area of the watershed. For streams that do not have gauging stations, flows were prorated from the nearest adjacent watershed with a flow gauging station. Example results are shown in Figures 22-23.

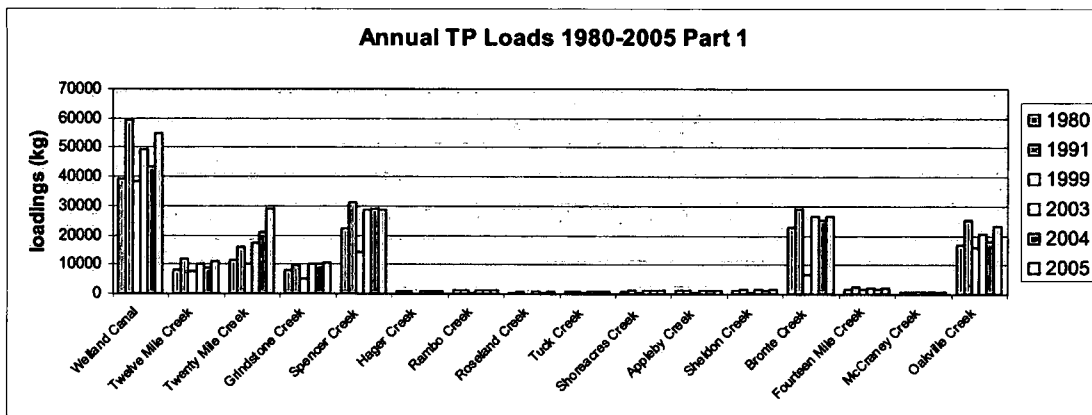


Figure 22: Event mean concentration annual total phosphorus loads for the period 1980-2005.

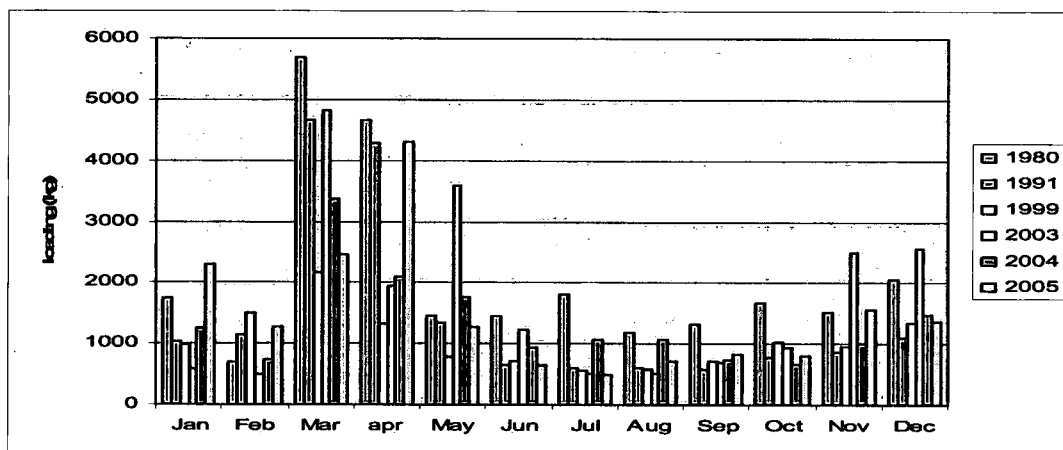


Figure 23: Duffins Creek Total Phosphorus Monthly EMC Loadings

5.3 MEASURED FLOWS AND CHEMISTRY METHODS

Where actual measured stream flow chemistry (e.g. the MOE enhanced PWQMN tributary stations in the 1990's, Conservation Authority) and flows were available for the study streams, actual loads were calculated as kg/yr, kg/ha/yr, and kg/ha/day. Two different loading calculation methods were used to deal with the issue of limited chemistry data. The Beale technique has been advocated for use since 1976 by the IJC. The Beale ratio indicator involves the relationship between two related populations, in this case flow and load. It assumes that the populations of flows and concentrations are approximately normally distributed, that the flows are monitored continuously and that discrete observations are available for the load population. A multi-strata technique is used to create more homogeneous subpopulations to more closely approach normality.

The NWRI technique assumes that flow is completely known and its errors can be ignored and that missing concentrations can be determined based upon the relationship between flow and concentration. The NWRI technique estimates the regression parameters by using the maximum likelihood or least square methods. Both techniques generate estimates of variance. Eddie and Onn, 1981 have shown that to achieve 10% precision for annual TP loads in Ontario streams, between 44 and 210 samples are required. An example is shown for the Niagara River for the period of 1992-2005 in Figure 24.

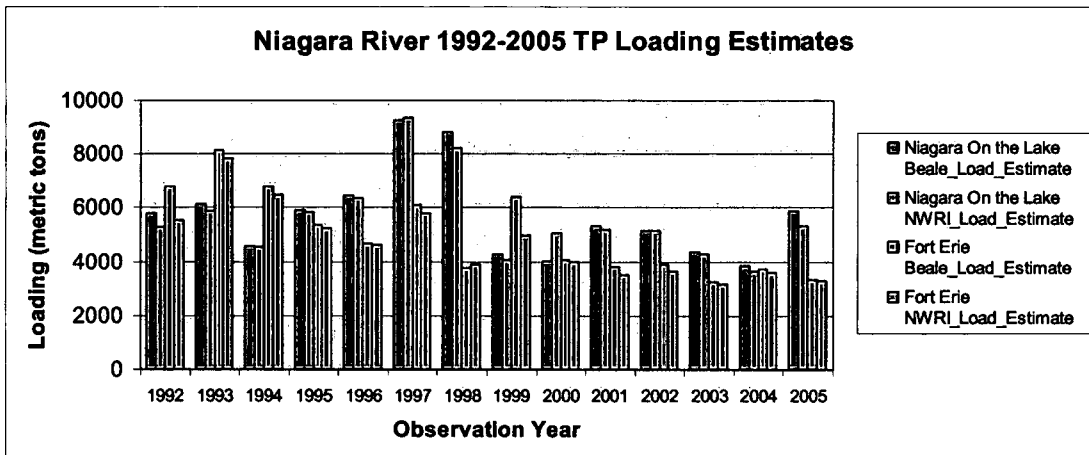


Figure 24: Niagara River TP loadings using the Beale and NWRI load estimate methods.

5.4 NON-POINT SOURCE LOAD MODELLING

The AGNPS non-point source model (Leon et al. 2004) was used to generate event loads for a number of different event scenarios, including extreme events (Booty et al., 2005). The AGNPS model requires inputs such as DEM, soil textures and land use. The DEM's were downloaded from NASA's Shuttle Radar Topography Mission SRTM web site "<http://www2.jpl.nasa.gov/srtm/dataproduct.htm>". The soil texture information was downloaded from the Canadian Soil Information System CanSIS web site and consists of GIS data (ARC/INFO EXPORT files) and soil reports. Land use data are from Provincial Land Cover 1998, County Official Plans, and AgCan: 2003 Landuse Coverage.

Scenarios of climate change were drawn from the Canadian Centre for Climate Modelling (CGCM2 model), where results are for the 2050s scenario relative to a 1961-1990 average. Results are also compared to current baseline conditions established for each watershed. The baseline storm events were typically in the range of 25-40 mm over a 12 hour period. It is well known now that the majority of the loads that enter the lake do so during a small number of major to extreme storm events. It is also predicted that the extreme storm events will become more frequent. For example, the Peterborough July 14th storm event generated 223 mm over a 12 hour period. This is used as an extreme event example to compare with the other baseline and climate change event scenarios. The results of running the ROS/AGNPS event model for these various scenarios for selected streams are shown in Figure 25. It can be seen that the Peterborough storm is predicted to generate almost an order of magnitude larger loadings than the baseline and climate change scenarios.

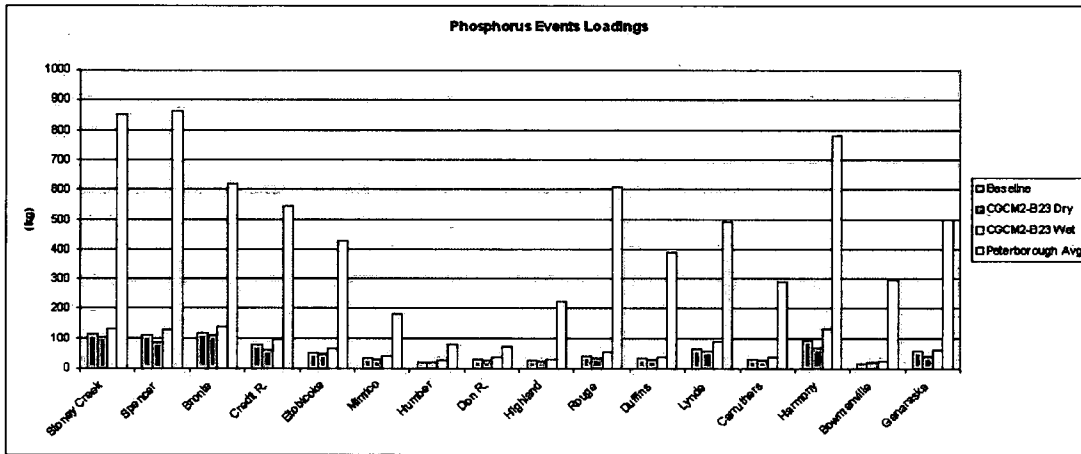


Figure 25: Comparison of various storm event scenarios for phosphorus loadings

Another extreme storm event that has been examined is the one that took place August 19th, 2005, in the Toronto region of Ontario. The storm exceeded the 100-year return period, with a morning event of 73 mm and an afternoon event of 62 mm. The ROS/AGNPS model has been used to predict loadings for three major streams entering Lake Ontario for this storm (135mm total) as compared to a baseline typical summer storm (25mm). The results are shown in Figures 26-28 for phosphorus, nitrogen and total suspended solids. This storm is predicted to generate from 1.7 to 12 times the load of phosphorus, 8.5 to 10 times the nitrogen, and 50 to 85 times the total dissolved solids compared to the baseline storm, depending on the watershed characteristics. In Figure 29, the MODIS satellite imagery before and after the storm showing the plumes generated in the Toronto area is shown. It can be seen that storms of this size can introduce enough nutrients and suspended solids into the lake to cause widespread changes in lake chemistry.

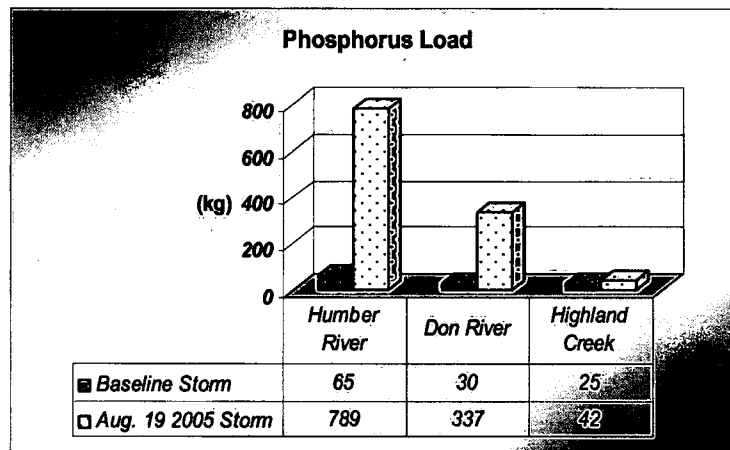


Figure 26: Comparison of baseline and Aug. 19 2005 storm phosphorus loads predicted using ROS/AGNPS model.

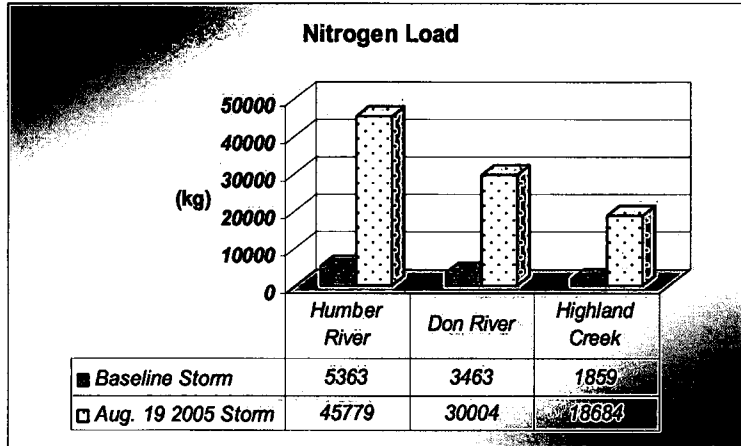


Figure 27: Comparison of baseline and Aug. 19 2005 storm nitrogen loads predicted using ROS/AGNPS model.

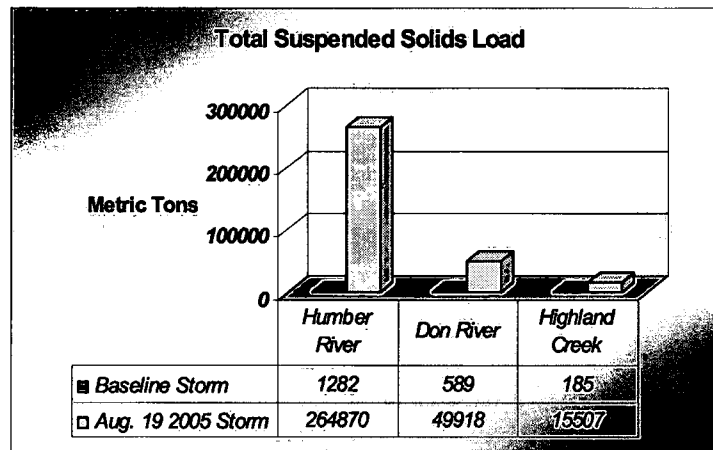


Figure 28: Comparison of baseline and Aug. 19 2005 storm total suspended solids loads predicted using ROS/AGNPS model.

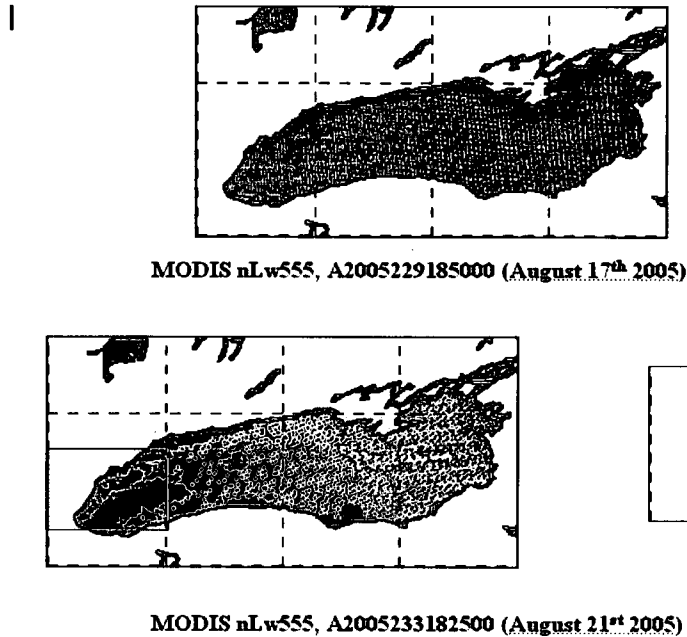


Figure 29: MODIS nLw555 imagery indicating general turbidity in Lake Ontario before and after the August 19th storm event.

In addition, our library of Landsat imagery was scanned to look for other potential storm generated plumes along the Lake Ontario shoreline. Below is a list of images that contained possible plumes for further study. Meteorological data files will be examined to determine if storms have taken place before or during these plumes.

UTM 18-30	1993 June 06
UTM 18-30	1985 Apr 29
UTM 18-29	1997 Jul 19
UTM 17-29	1994 Jun 18
UTM 17-29	1991 Apr 07
UTM 17-29	1998 Apr 10
UTM 17-29	1987 May 30
UTM 17-29	1986 May 11
UTM 17-29	1986 Aug 31
UTM 16-29	1986 Jul 23

6 COMMUNICATIONS

Papers in peer-reviewed journals, presentations at conferences, workshops and departmental seminars, collaborations & direct contact with end-users have been used to advance knowledge of applications of satellite-derived water quality products.

Wealth of Water Publications/Invited Presentations to date:

- Bukata, R.P., Jerome, J.H., Borstad, G.A., Brown, L.N., and Gower, J.F.R. 2003. Developing useful water quality products from hyperspectral satellite imagery: Some early lessons from MODIS and WATERS data. *Backscatter*, Winter issue, 29-31.
- Bukata, R.P. and Jerome, J.H. 2003. Water quality from inland water colour: Some pros and cons of multivariate bio-optical modeling and optimization. Invited paper at the combined Scientific Conferences of the Alliance for Marine Remote Sensing (AMRS) and The Oceanographic Society (TOS), New Orleans.
- Bukata, R.P. and Jerome, J.H. 2003. Water colour observed from satellite altitudes: A contribution to inland water quality modeling. Solicited by the Paris, France Water Business Magazine HYDROPLUS, Hydroplus, Hydrosiences, 132, 61-64.
- Jerome, J.H. 2003. Application of remote sensing to nearshore dynamics of southeastern Lake Huron. Invited presentation to the Lake Huron SE Shore Working Group.
- Bukata, R.P. and Helbig, J.A. 2004. Monitoring coastal ocean and inland water quality from hyperspectral water color. *Backscatter*, Winter issue, 33-37.
- Bukata, R.P., Jerome, J.H., Borstad, G.A., Brown, L.N., and Gower, J.F.R. 2004. Mitigating the impact of trans-spectral processes on multivariate retrieval of water quality parameters from case 2 waters. *Canadian Journal of Remote Sensing*, 30, 8-16.
- Gower, J.F.R. 2004. SeaWiFS global composite images show significant features of Canadian waters for 1997-2001. *Canadian Journal of Remote Sensing*, 30, 26-35.
- Bukata, R.P. 2005. *Satellite Monitoring of Inland and Coastal Water Quality: Retrospection, Introspection, Future Directions*. Hard cover book solicited by Taylor & Francis/CRC Press, Boca Raton, FL, 272 pages.
- Jerome, J.H. 2005. Satellite observations of Lake Ontario during taste-and-odor events. Invited presentation to the Ontario Water Works Research Consortium Workshop.
- Binding, C.E., Jerome, J.H., Booty, W.G., and Bukata, R.P. 2005. Inland water quality from space. Poster presented at Canadian Space Agency's InfoDays.
- Bukata, R.P. 2006. End-users of satellite-derived water quality products: A reality check. Invited plenary talk at the 5th Annual NY State Remote Sensing Symposium/Great Lakes Regional Data Exchange Conference, Rochester, N.Y.
- Bukata, R.P. 2006. Remote monitoring of the Great Lakes. Invited commentary, *Advisor*, Great Lakes Commission publication, 9-10.
- Booty, W.G. Non-point source water quality modeling. Invited presentation, Remedial Action Plan Implementer's Workshop, Guelph, Ontario, Jan. 26-27, 2006.
- Bukata, R.P., "Relating Satellite Observations of Water Colour to Water Quality and Land-use in the Great Lakes Basin", presentation at the EC Space-Based Monitoring Workshop, Dec 5-6, 2006.
- Bukata, R.P., Binding, C.E., Jerome, J.H., Booty, W.G., and Lawrence, J., "A Wealth of Water: Relating Water Quality Products from Satellite Observations of Inland Water Colour to Land Use in the Laurentian Great Lakes Drainage System", presentation at the EC Space Based Outcome Project Plan Workshop, Dec. 5-6, 2006.
- Booty, W.G., Bukata, R.P., Binding, C.E., and Jerome, J.H. Integrated Modeling of Water Quality using Satellite and Land-based Non-Point Source Models in Canada, *International Symposium for Environmental Software Systems*, ISESS 2007, May 2007, Prague, Czech Republic.

- Booty, W.G. and Bowen, G.S., "Determination of Tributary Nutrient Loadings on the Canadian Side of Lake Ontario", presented in the "Eutrophication Management in the Great Lakes: How Did We Do It in the Past and Where Should We Go in the Future?" session, International Association for Great Lakes Research Conference, Penn State University, June 1, 2007.
- Binding, C. E., Jerome, J. H., Bukata, R. P. and Booty, W. G. 2007. Trends in water clarity of the Great Lakes from SeaWiFS aquatic colour. *Journal of Great Lakes Research*, 33:828-841.
- Binding, C. E., Jerome, J. H., Bukata, R. P. and Booty, W. G. 2008. The impact of dissolved organic matter on particulate spectral absorption properties of inland waters. *Remote Sensing of Environment*, 112:1702-1711.
- Binding, C. E. Trends in water clarity of the lower Great Lakes from remotely sensed aquatic colour. 43rd Central Canadian Symposium on Water Quality Research. Burlington, Ontario, Feb.11-12, 2008.
- Jerome, J.H., Binding, C.E., Bukata, R.P., Stainton, M.P., McCullough, G.K. Optical properties, water colour, and water quality of Lake Winnipeg. Lake Winnipeg Research Consortium Science Workshop. Winnipeg, Manitoba. March 17-19, 2008.
- Binding et al. Suspended particulate matter in Lake Erie derived from MODIS aquatic colour imagery. In prep.
- Binding et al. Satellite monitoring of algal blooms in Canadian inland waters. In prep

7 THE FUTURE

On the basis of the results obtained during the Wealth of Water GRIP project, logical continuation of scientific activities would include:

- Rendering image processing & water quality product mapping operational
- Further development and validation of algal bloom flag & chlorophyll mapping
- Incorporate MERIS imagery into NWRI's water quality monitoring program
- Demonstrate versatility by capitalizing on satellite capabilities of monitoring harmful algal blooms

8 SUMMARY & CONCLUSIONS

To summarize, the project WOW made significant advancements in the application of remote sensing technologies to routine environmental monitoring of the Great Lakes, producing observations of water quality (including water clarity, suspended particulates and algal blooms) that directly contribute to Environment Canada's mandates to monitor and protect freshwater quality. Specifically, the outcomes of the project were:

- Comprehensive data sets of optical properties and water quality parameters for Lakes Ontario, Erie and Winnipeg
- Extensive archive of satellite aquatic colour imagery of the Great Lakes from MODIS, SeaWiFS, CZCS, MERIS & Landsat
- The generation of time-series maps of water clarity, suspended particulates, (and tentatively, algal blooms) over the lower Great Lakes
- Successful application and validation of NWRI optical models for the retrieval of water quality parameters
- Archive of ground-base data for non-point source modelling of Canadian Lake Ontario watersheds
- Demonstration of the impact of land-based processes on lake chemistry as observed by satellites

REFERENCES

- Amos, C. L. and Topliss, B. J. 1985. Discrimination of suspended particulate matter in the Bay of Fundy using the Nimbus-7 Coastal Zone Colour Scanner. *Canadian Journal of Remote Sensing*, Vol. 11, pp.85-92.
- Aquafor Beech, 2005. LOSAAC Water Quality Study, Prepared for Conservation Halton, Aquafor Beech Reference: 64353.
- Aufdenkampe, A. K., J. I. Hedges, J. E. Richey, A. V. Krusche, and C. A. Llerena. 2001. Sorptive fractionation of dissolved organic nitrogen and amino acids onto fine sediments within the Amazon basin. *Limnol. Oceanogr.* 46: 1921-1935.
- Austin, R. W. 1974. The remote sensing of spectral radiance from below the ocean surface. In: Jerlov, N. G. and Nielsen, E. S (Eds) *Optical Aspects of Oceanography* (Chapter 14, pp. 317-344). London: Academic Press. 494pp.
- Babin, M., D. Stramski, G. M. Ferrari, H. Claustre, A. Bricaud, G. Obolensky, and N. Hoepffner. 2003. Variations in the light absorption coefficients of phytoplankton, nonalgal particles, and dissolved organic matter in coastal waters around Europe. *J. Geophys. Res.* 108, C7, doi:10.1029/2001JC000882
- Baith, K., R. Lindsay, G. Fu, and C.R. McClain. 2001: SeaDAS, a data analysis system for ocean-color satellite sensors. *EOS Trans. AGU*, 82. pg 202
- Barbiero, R. P. and M. L. Tuchman. 2004. Long-term Dreissenid Impacts on Water clarity in Lake Erie. *J. Great Lakes Res.* 30(4): 557-565.
- Binding, C. E., Jerome, J. H., Bukata, R. P. and Booty, W.G. 2008. Spectral absorption properties of dissolved and particulate matter in Lake Erie. *Remote Sensing of Environment*, 112:1702-1711.
- Binding, C. E., Bowers, D. G. and Mitchelson-Jacob, E.G. 2003. An algorithm for the retrieval of suspended sediment concentrations in the Irish Sea from SeaWiFS ocean colour satellite imagery. *International Journal of Remote Sensing*, Vol. 24, No. 19, pp. 3791-3806.
- Binding, C. E., Jerome, J. H., Bukata, R. P. and Booty, W.G. 2007. Trends in water clarity of the lower Great Lakes from remotely sensed aquatic colour. *Journal of Great Lakes Research*, 33:828-841.
- Booty, W.G., Lam, D.C.L., Bowen, G.S., Resler, O, and Leon, L. 2005. Modelling Changes in Streamwater Quality due to Climate Change in a Southern Ontario Watershed. *Canadian Water Resources Journal* Vol. 30 (3):211-226.
- Bowers, D. G., G. E. L. Harker, and B. Stephan. 1996. Absorption spectra of inorganic particles in the Irish Sea and their relevance to remote sensing of chlorophyll. *Int. J. Remote Sens.* 17: 2449-2460.
- Bricaud, A., M. Babin, A. Morel, and H. Claustre. 1995. Variability in the chlorophyll-specific absorption coefficients of natural phytoplankton: Analysis and parameterization. *J. Geophys. Res.* 100: 13,321-11,332.
- Bukata, R. P. 2005. *Satellite monitoring of inland and coastal water quality; retrospection, introspection, future directions*. CRC Press. 246pp.
- Bukata, R. P., J. E. Bruton, and J. H. Jerome. 1983. Use of chromaticity in remote measurements of water quality. *Remote Sens. Environ.* 13: 161-177.
- Bukata, R. P., J. H. Jerome, J. H. Bruton, S. C. Jain, and H. H. Zwick. 1981. Optical water quality model for Lake Ontario: 2. Determination of chlorophyll a and suspended mineral concentrations of natural waters from submersible and low altitude optical sensors. *Appl. Opt.* 20: 1704-1714.
- Bukata, R. P., J. H. Jerome, K. Ya. Kondratyev, and D. V. Pozdnaykov. 1991. Estimation of organic and inorganic matter in inland waters: Optical cross sections of Lakes Ontario and Ladoga. *J. Great Lakes Res.* 17: 461-469.

- Bukata, R. P., J. H. Jerome, K. Ya. Kondratyev, and D. V. Pozdnaykov. 1995. *Optical Properties and Remote Sensing of Inland and Coastal Waters*. CRC Press, Boca Raton, FL, 362 pp.
- Carder, K. L., R. G. Steward, G. R. Harvey, and P.B. Ortner. 1989. Marine humic and fulvic acids: their effects on remote sensing of ocean chlorophyll. *Limnol. Oceanogr.* 34: 68-81.
- Charlton, M.N. and Lean, D.R.S. 1987. Sedimentation, resuspension and oxygen depletion in Lake Erie (1979). *Journal of Great Lakes Research*, 13(4):709-723.
- City of Toronto Wet Weather Flow, Humber River HSPF Water Quality and Stormwater Management Study.
- Corsi, S.R., Graczyk, D.J., Owens, D.W., and Bannerman, R.T. Unit Area Loads of Suspended Sediment, Suspended Solids, and Total Phosphorus from Small Watersheds in Wisconsin, USGS Fact Sheet FS-195-97.
- Dodd, R.C., McMahon, G. and Stichter, S. 1992. Watershed planning in the Abermarle-Pamlico estuarine system, Report1 –annual average nutrient budgets. Report No. 92-10. Albermarle-Pamlico Estuarine Study, NC Department of Environment, Health and Natural Resources, Raleigh, NC.
- Eddie, J.D. and Onn, D.F. 1981. Enhanced Great Lakes Tributary Monitoring in Ontario: 1980 Water Quality Status Report, Hydrology and Monitoring Section, Ontario Ministry of the Environment, Water Resources Paper 16.
- Environment Canada. 1997. Manual of Analytical Methods, Volume 3, Organics. Environmental Conservation Service - ECD. Canadian Communications Group. Toronto, Ont.
- Environment Canada. 2001. Threats to sources of drinking water and aquatic ecosystem health in Canada. National Water Research Institute, Burlington, Ontario. NWRI Scientific Assessment Report Series No. 1, 72p.
- Hamdy, Y. and Post, L. 1985. Distribution of mercury, trace organics, and other heavy metals in Detroit River sediments. *J. Great Lakes Res.* 11 (1985), pp. 353–365.
- Hawley, N. and Eadie, B. J. 2007. Observations of sediment transport in Lake Erie during the Winter of 2004-2005. *Journal of Great lakes Research*, 33:816-827.
- International Reference Group on Great Lakes Pollution from Land Use Activities. 1976. *Agricultural Watershed Studies in the Canadian Great Lakes Drainage Basin*.
- Jerome, J. H., Bukata, R. P. and Bruton, J. E. 1988. Utilizing the components of vector irradiance to estimate the scalar irradiance in natural waters. *Applied Optics*, 27: 4012-4018.
- Kemp, A.L.W., MacInnis, G. A. and Harper, N.S. 1977. Sedimentation rates and a revised sediment budget for Lake Erie. *Journal of Great lakes Research*, 3(3-4):221-233.
- Kirk, J.T.O, 1994. *Light and Photosynthesis in Aquatic Ecosystems 2nd ed.* Cambridge University Press, U.K. 509 pp.
- Leon, L.F., Booty, W.G., Bowen, G.S., and Lam, D.C.L. 2004. Validation of an agricultural non-point source model in a watershed in southern Ontario. *Agricultural Water Management* 65: 59-75.
- Makarewicz, J. C., T. W. Lewis and P. Bertram. 1999. Phytoplankton composition and biomass in the offshore waters of Lake Erie: pre- and post-*Dreissena* introduction (1983-1993). *J. Great Lakes Res.*, 25:135-148.
- Marvin, C.H., Charlton, M.N., Reiner, E.J., Kolic, T., MacPherson, K., Stern, G.A., Braekevelt, E., Estenik, J.F., Thiessen, L. and Painter, S.. 2002. Surficial sediment contamination in lakes Erie and Ontario: A comparative analysis. *Journal of Great Lakes Research*. 28(3): 437–450.

- McClain, C.R., G.C. Feldman, and S.B. Hooker. 2004. An overview of the SeaWiFS project and strategies for producing a climate research quality global ocean bio-optical time series. *Deep Sea Res. II*, 51, 5-42
- MOE/EC Large Volume Sampling at Six Lake Ontario Tributaries During 1997 and 1998: Project Synopsis and Summary of Selected Results, 1999, ISBN 0-7778-9257-X.
- Morel, A. and Gentili, B. 1996. Diffuse reflectance of oceanic waters. III. Implication of bidirectionality for the remote sensing problem. *Applied Optics*, 35:4850-4862.
- Morel, A. and Mueller, J. L. 2003. Normalized water-leaving radiance and remote sensing reflectance: bidirectional reflectance and other factors. In J. L. Mueller, G.S. Fargion, and C. R. McClain. *Ocean Optics Protocols for Satellite Ocean Color Sensor validation, Revision 4, Volume III: Radiometric Measurements and Data Analysis Protocols. NASA/TM-2003-211621 Rev4-Vol.III.*
- Morel, A., and H. Loisel. 1998. Apparent optical properties of oceanic water: dependence on the molecular scattering contribution. *Appl. Opt.* 37: 4765-4776.
- Morel, A., and L.Prieur. 1977. Analysis of variations in ocean colour. *Limnol. Oceanogr.* 22: 709-721.
- Novo, E. M. M., Hansom, J. D. and Curran, P. J. 1989. The effect of sediment type on the relationship between reflectance and suspended sediment concentration. *International Journal of Remote Sensing*, Vol. 10, No. 7, pp. 1283-1289.
- Ostry, R.C. and Tseng, T. 1981. A Preliminary Method for Evaluation of Non-Point Sources: An Assessment Procedure for Working Group II of the Water Management Steering Committee. The Ontario Ministry of Environment, Toronto, Ontario.
- Painter, S., Marvin, C.H., Rosa, F., Reynoldson, T., Charlton, M.N., Fox, M., Thiessen, P.A. and Eestnik, J.F. 2001. Sediment contamination in Lake Erie: A 25-year retrospective analysis. *Journal of Great Lakes Research*. 27(4): 434-448.
- Petzold, T. J. 1972. Volume scattering functions for selected ocean waters. In: *Light in the Sea*, Edited by Tyler, J. E. Dowden, Hutchinson & Ross, Stroudsburg. pp. 150-174.
- Robinson, M. C., Morris, K. P. and Dyer, K. R. 1998. Deriving fluxes of suspended particulate matter in the Humber Estuary, UK, using airborne remote sensing. *Marine Pollution Bulletin*, Vol. 37, No. 3-7, pp. 155-163.
- Rukavina, N. A. and Zeman, A.J. 1987. Erosion and sedimentation along a cohesive shoreline – the north-central shore of Lake Erie. *Journal of Great Lakes Research*, 13(2):202-217.
- Shank, G. C., R. G. Zepp, R. F. Whitehead, and M. A. Moran. 2005. Variations in the spectral properties of freshwater and estuarine CDOM caused by partitioning onto river and estuarine sediments. *Estuar. Coast. Shelf S.* 65: 289-301.
- Smith, R. E. H., Parrish, C. C., Depew, D. C. and Ghadouani, A. 2007. Spatial patterns of seston concentration and biochemical composition between nearshore and offshore waters of a Great Lake. *Freshwater Biology*, 52:2196-2210.
- Stantec/Aquafor Beech Consulting, 2003. Dry and Wet Weather Modelling of Water Quality Under Alternative Land Use Scenarios in the Duffins and Carruthers Creek Watersheds: A Simple Approach, Prepared for The Toronto and Region Conservation Authority, Project No. 631 22714.1
- Surface Water Monitoring and Assessment 1997 Lake Ontario Report: Featuring a Summary of tributary and Nearshore Conditions and Trends for the Lake Ontario Basin, Environmental Monitoring and Reporting Branch, November 1999, Queen's Printer for Ontario, ISBN 0-7778-9531-5.
- Topliss, B. J. 1986. Spectral variations in upwelling radiant intensity in turbid coastal waters. *Estuarine, Coastal and Shelf Science*, Vol. 22, pp. 395-414.
- TRCA Surface Water Quality Conditions of Streams in the Toronto RAP Watershed Report, Feb., 2001.

- Winter, J., Dillon, P., Futter, M., Nicholis, K., Schneider, W. and Scott, L. 2002. Total phosphorus budgets and nitrogen loads: Lake Simcoe, Ontario (1990 to 1998), Journal of Great Lakes Research. 28(3):301-314.
- Zepp, R. G., and P. F. Schlotzhauer. 1981. Comparison of photochemical behaviour of various humic substances in water: 3. Spectroscopic properties of humic substances. Chemosphere 10: 479-486.

APPENDICES

Appendix 1

Table 1.1 Tributaries examined for loadings in this study

Stream Name	WSC Station	Total Drainage Area (ha)
Welland Canal	02HA019	9900
Twelve Mile Cr.		11900
Twenty Mile Cr.	02HA006	31400
Redhill Cr.	02HA014	10452
Grindstone Cr.	02HB012	12521
Spencer Cr.	02HB007	27955
Hager Cr.		899
Rambo Cr.		1480
Roseland Cr.		740
Tuck Cr.		1065
Shoreacres Cr.		1405
Appleby Cr.		1467
Sheldon Cr.		1720
Bronte Cr.	02HB011/02HB022	30491
Fourteen Mile Cr.	02HB027	3500
McCraney Cr.		1500
Oakville/Sixteen Mile Cr.	02HB004	37400
Morrison Cr.		500
Wedgewood Cr.		600
Joshua's Cr.		2100
Credit River	02HB001	93804
Etobicoke Cr.	02HC030	22382
Mimico Cr.	02HC033	8822
Humber River	02HC003	91303
Don River	02HC024	38383
Highland Cr.	02HC013	11446
Rouge River	02HC022	38795
Duffins Creek	02HC006/02HC049	28564
Lynde Creek	02HC018	16856
Carruthers Cr.		4207
Oshawa Cr.	02HD008	26675
Harmony Cr.	02HD013	20247
Bowmanville Cr.	02HD006	29934
Soper Cr.	02HD007	
Wilmont Cr.	02HD007	14600
Graham Cr.		9300
Ganaraska River	02HD012	34840
Gage Creek		4860
East of Gage Cr. tribs		1250
Cobourg Cr.		22890

Brookside Cr.		
Barnum House Cr.		
Grafton Cr.		
Colborne Cr.		
Salem Cr.		
Butler Cr.		
Smithfield Cr.		

Appendix 2.

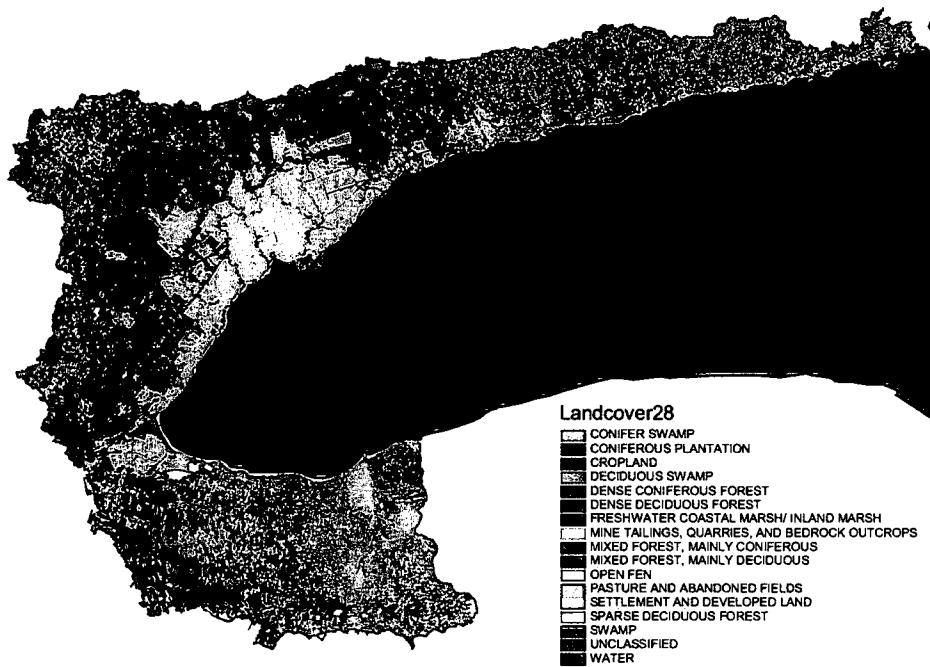


Figure 2.1 Land cover classification map for study area

Canada Centre for Inland Waters

P.O. Box 5050
867 Lakeshore Road
Burlington, Ontario
L7R 4A6 Canada

National Hydrology Research Centre

11 Innovation Boulevard
Saskatoon, Saskatchewan
S7N 3H5 Canada

St. Lawrence Centre

105 McGill Street
Montreal, Quebec
H2Y 2E7 Canada

Place Vincent Massey

351 St. Joseph Boulevard
Gatineau, Quebec
K1A 0H3 Canada

Centre canadien des eaux intérieures

Case postale 5050
867, chemin Lakeshore
Burlington (Ontario)
L7R 4A6 Canada

Centre national de recherche en hydrologie

11, boul. Innovation
Saskatoon (Saskatchewan)
S7N 3H5 Canada

Centre Saint-Laurent

105, rue McGill
Montréal (Québec)
H2Y 2E7 Canada

Place Vincent-Massey

351 boul. St-Joseph
Gatineau (Québec)
K1A 0H3 Canada



Environment
Canada

Environnement
Canada

Canada